EUROPEAN ORGANIZATION FOR NUCLEAR RESEARCH

CERN-EP-2000-153
December 19, 2000

Combination procedure for the precise determination of Z boson parameters from results of the LEP experiments

The LEP Collaborations ALEPH, DELPHI, L3 and OPAL [1] and
the Line Shape Sub-group of the LEP Electroweak Working Group [2]

Abstract

The precise determination of the Z boson parameters from the measurements at the Z resonance by the four collaborations ALEPH, DELPHI, L3 and OPAL in e^+e^- collisions at the large electron positron collider LEP at CERN is a landmark for precision tests of the electroweak theory. The four experiments measured quantities which were used to extract the mass and width of the Z boson, the hadronic cross-section at the pole of the resonance, the ratio of hadronic and leptonic decay widths, and the leptonic forward-backward asymmetries at the pole. The combination procedure based on these parameters is presented in this paper.

(to be published as part of a review in Physics Reports)

[1] The full list of authors may be found in References 1–4

[2] The members of the line shape group are: G. Duckeck, M. Grünewald, T. Kawamoto, R. Kellogg, G. Martinez, J. Mnich, A. Olshevski, B. Pietrzyk, G. Quast, P. Renton, E. Tournefier

1 Introduction

Between the years 1989 and 1995 the e^+e^- collider LEP at CERN provided interactions at centre-of-mass energies, $\sqrt{s}$, ranging from 88 to 95 GeV, *i.e.* around the mass of the Z boson (LEP I phase). An important aspect of physics at LEP concerns the analysis of fermion-pair production in e^+e^- collisions [5]. The four LEP experiments ALEPH [6], DELPHI [7], L3 [8] and OPAL [9] analysed, in particular, hadron (quark-pair) production and the pair production of charged leptons, $\ell = \mathrm{e}, \mu, \tau$.

At various centre-of-mass energies, total cross-sections are measured for all processes, while forward-backward asymmetries are measured in lepton-pair production. These measurements ("*realistic observables*") allow the determination of various properties of the Z boson such as its mass, total and partial decay widths, and coupling constants to fermions ("*pseudo-observables*"). For the extraction of the pseudo-observables, the experiments perform model-independent fits to their measured realistic observables [1–4].

To obtain the best possible precision the results of the four LEP experiments have to be averaged. This paper describes the combination procedure adopted by the LEP electroweak working group. Performing an average over the realistic observables constitutes an extremely complicated task, as it involves hundreds of measurements, each with specific phase space definitions and experimental errors which are correlated among different centre-of-mass energies and data taking periods and also among the LEP experiments. Therefore, the combination of the experimental results is performed on the basis of the four sets of pseudo-observables. As will be shown here, this is possible without significant loss of precision.

Additional fits to the experimental data, usually not contained in the individual publications quoted above, were provided by the experiments and are documented in this paper. A large effort is devoted to the treatment of systematic errors and their correlation among the experiments, such that the combination procedure yields an optimal estimator for the averages.

This paper is organised as follows: Section 2 summarises the information about the LEP I running relevant for this paper. Section 3 presents a brief introduction to the pseudo-observables used to parametrise the realistic observables around the Z resonance. The individual experimental results are presented in Section 4. Sources of correlated systematic errors between experiments and their effects on the pseudo-observables are discussed in Section 5. In Section 6, studies of various methods for combining the results are presented. The resulting pseudo-observables are then considered in the framework of a specific model, the minimal Standard Model (SM), and are compared with direct SM fits to the realistic observables. The conclusions are summarised in Section 7.

2 Z resonance scans at LEP I

Running of LEP in the years from 1989 to 1995 was dedicated to precision studies of the Z boson parameters. Electron-positron collisions were provided at several well-determined centre-of-mass energies around the Z resonance, with steadily improving performance. The set of measurements collected by the experiments consists of the hadronic and leptonic cross-sections and the leptonic forward-backward asymmetries around seven points in centre-of-mass energy, over six years of running at LEP I. In addition, changes of experimental conditions, such as the inclusion of new detector components, made it necessary to subdivide the data samples even further. The full LEP I data set consists of about 4×200 individual cross-section and asymmetry measurements. From these each experiment has extracted a set of parameters describing the cross-section around the Z resonance, which include the mass, m_{Z}, and width, Γ_{Z}, of the Z and the total pole cross-section for $\mathrm{q\overline{q}}$ production, σ^0_{h}. These parameters are discussed in detail in Section 3 . QED corrections from initial-state photon radiation are large around the Z resonance due to the rapid variation of the cross-sections with centre-of-mass energy. For illustration, Figure 1 shows the average over the hadronic cross-section measurements by the four experiments, together with the fitted line shape curve before and after unfolding photon radiation. The cross-section is dominated by on-shell Z production, although photon exchange and γ-Z interference contributions are not negligible. The measurements are sensitive to higher-order electroweak corrections. These modify the tree-level couplings of the Z to fermions, and are quantified in terms of electroweak form factors.

Much effort was dedicated to the determination of the energy of the colliding beams, which reached a precision of about 20×10^{-6} on the absolute energy scale. This level of accuracy is vital for the measurements of the mass and width of the Z. All the experiments replaced their first-generation luminosity detectors, which had systematic uncertainties around the percent level, by high-precision devices capable of pushing systematic errors on the acceptance of small-angle Bhabha scattering events below one per-mil. As a consequence of improvements of the accelerator and of the experiments during LEP I running, statistical and systematic errors are much smaller for the last three years of data taking, which hence dominate the precision achieved on the Z parameters.

2.1 Event selection and statistics

During the summer of 1989 the first Z bosons were produced at LEP and observed by the four experiments. Since then the operation of the machine and its performance were steadily improved. At the end of data taking around the Z resonance in autumn 1995 the peak luminosity had reached nearly twice its design value. Table 1 summarises the data taking periods, the approximate centre-of-mass energies and the integrated luminosities delivered.

The data collected in 1989 constitute only a very small subset of the total statistics and are of lower quality, and therefore are not used here. In the years 1990 and 1991 "energy scans" were performed at seven different centre-of-mass energies around the peak of the Z resonance, placed about one GeV apart. In 1992 and 1994 there were high-statistics runs at the peak energy only. In 1993 and 1995 data taking took place at three energy points, about 1.8 GeV below and above the peak and at the peak. In particular the off-peak energies were carefully calibrated employing the technique of resonant depolarisation of the

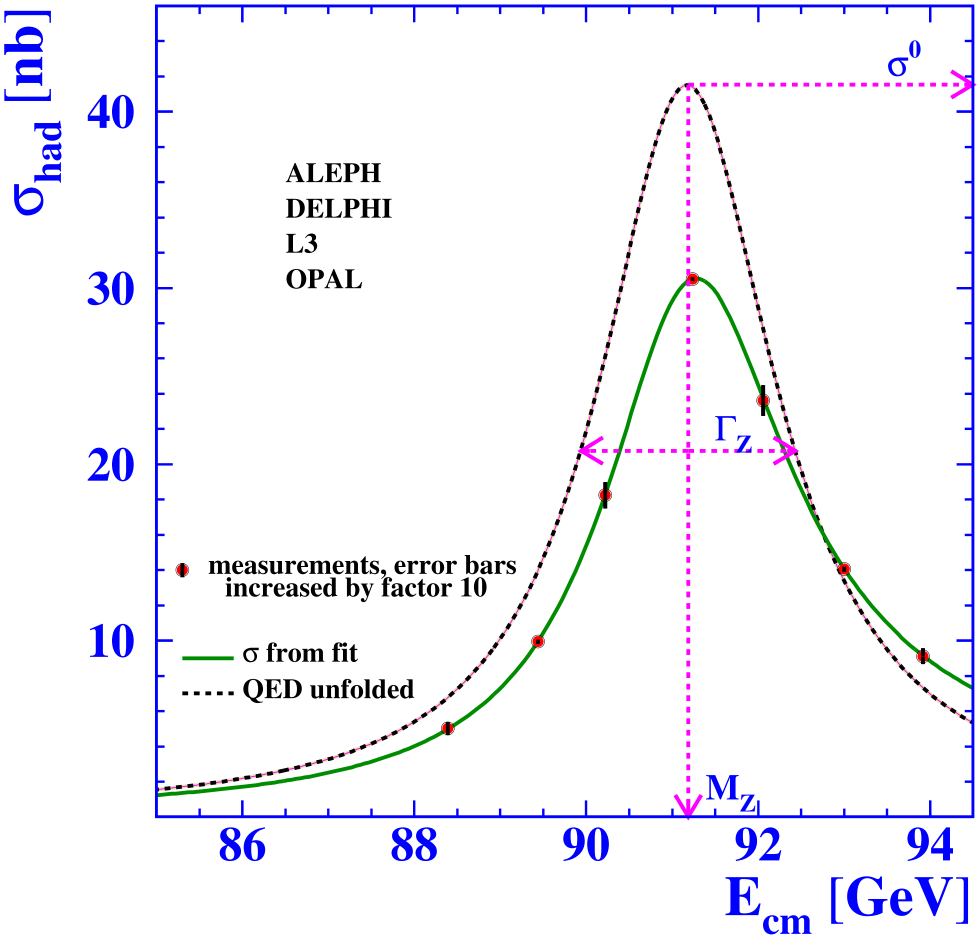

Figure 1: *Average over measurements of the hadronic cross-sections by the four experiments, as a function of centre-of-mass energy. The dashed curve shows the QED deconvoluted cross-section, which defines the Z parameters described in the text.*

transversely polarised beams [10–13].

The accumulated event statistics amount to about 17 million Z decays recorded by the four experiments. A detailed breakdown is given in Table 2.

As an example, the measurements of the hadronic cross-section at the three principal energy points are shown in Figure 2. Because the hadron statistics are almost ten times larger than the lepton statistics, these measurements dominate the determination of the mass and the width of the Z. Detailed descriptions of the individual experimental analyses can be found in [1–4]. They all rely on excellent separation of the final states, $q\overline{q}$, e^+e^-, $\mu^+\mu^-$ and $\tau^+\tau^-$, accompanied by high selection efficiencies. The total cross-section, $\sigma_{\rm tot}$, is determined from the number of selected events in a final state, N, the number of background events, $N_{\rm bg}$, the selection efficiency, ϵ, and the integrated luminosity, $\mathcal{L}$, as $\sigma_{\rm tot} = (N - N_{\rm bg})/(\epsilon\mathcal{L})$.

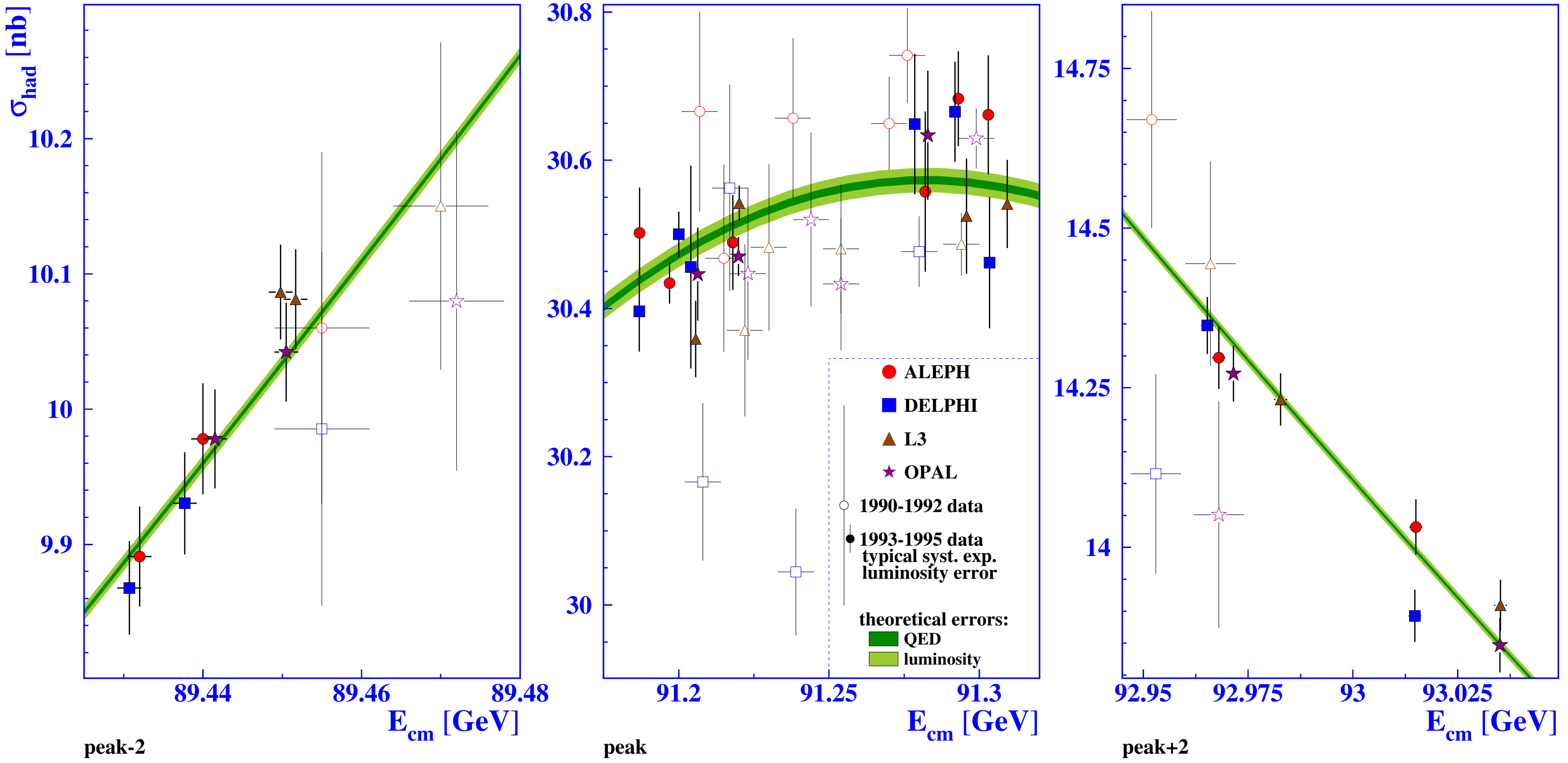

Figure 2: *Measurements by the four experiments of the hadronic cross-sections around the three principal energies. The vertical error bars show the statistical errors only. The open symbols represent the early measurements with typically much larger systematic errors than the later ones, shown as full symbols. Typical experimental systematic errors on the determination of the luminosity are indicated in the legend; these are almost fully correlated within each experiment, but uncorrelated among the experiments. The horizontal error bars show the uncertainties in* LEP *centre-of-mass energy, where the errors for the period 1993–1995 are smaller than the symbol size in some cases. The bands represent the result of the model-independent fit to all data, including the two most important common theoretical errors from initial-state photon radiation and from the calculations of the small-angle Bhabha cross-section.*

year	beam energy range [GeV]	integrated luminosity [pb^{-1}]
1989	[88.2 , 94.2]	1.7
1990	[88.2 , 94.2]	8.6
1991	[88.5 , 93.7]	18.9
1992	91.3	28.6
1993	89.4, 91.2, 93.0	40.0
1994	91.2	64.5
1995	89.4, 91.3, 93.0	39.8

Table 1: *Approximate centre-of-mass energies and integrated luminosities delivered by* LEP*, per experiment. In 1990 and 1991, a total of about 7 pb^{-1} was taken at off-peak energies, and 20 pb^{-1} per year in 1993 and in 1995. The total luminosity used by the experiments in the analyses was smaller by 10-15 % due to data taking inefficiencies.*

	q$\overline{\text{q}}$					$\ell^+\ell^-$				
year	A	D	L	O	all	A	D	L	O	all
'90/91	433	357	416	454	1660	53	36	39	58	186
'92	633	697	678	733	2741	77	70	59	88	294
'93	630	682	646	649	2607	78	75	64	79	296
'94	1640	1310	1359	1601	5910	202	137	127	191	657
'95	735	659	526	659	2579	90	66	54	81	291
total	4071	3705	3625	4096	15497	500	384	343	497	1724

Table 2: *The* q$\overline{\text{q}}$ *and* $\ell^+\ell^-$ *event statistics, in units of* 10^3*, used for the analysis of the Z line shape and lepton forward-backward asymmetries by the experiments* ALEPH *(A),* DELPHI *(D),* L3 *(L) and* OPAL *(O).*

The luminosity of the beams is determined by normalisation to the theoretical cross-section for the process of small-angle Bhabha scattering, which is dominated by photon exchange in the t channel. Thus, the integrated luminosity is given by the number of observed small-angle Bhabha events and the calculated cross-section for this process within a given experimental acceptance. This requires the detection of back-to-back electrons and positrons close to the beam direction. Their positions and energies are precisely measured by forward calorimeters placed at small angles with respect to the beam line (typically 30 mrad$< \theta <$50 mrad). The main experimental systematic error arises from the definition of the geometrical acceptance for this process. Since the angular distribution is steeply falling with increasing scattering angle ($\propto \theta^{-3}$), the precise definition of the inner radius of the acceptance region is most critical.

The forward-backward asymmetry, A_{fb}, is defined by the numbers of events in which the final state lepton goes forward or backward with respect to the direction of the incoming electron, N_f and N_b, respectively: $A_\mathrm{fb} = (N_\mathrm{f} - N_\mathrm{b})/(N_\mathrm{f} + N_\mathrm{b})$. In practice, A_fb is determined from a fit to the differential cross-section of the form $d\sigma/d\cos\theta \propto 1 + \cos^2\theta + {}^8/_3\, A_\mathrm{fb} \cos\theta$, where θ is the angle between the direction of the final state fermion and that of the incoming electron. This procedure makes better use of the available information and hence leads to slightly smaller statistical errors. The electron final state is special due to t-channel diagrams, as is discussed in more detail in Section 5.2. The forward-backward asymmetries do not require any normalisation, but rely on precise measurements of the production angles of the final state fermions. Forward-backward asymmetries in $\mathrm{q\overline{q}}$ final states are not considered here, because these require either dedicated techniques for the tagging of quark flavours or a special method to extract the inclusive quark forward-backward asymmetry from the natural mixture of quark flavours in hadronic events.

In general, the systematic errors arising from the selection procedures are small and so the accumulated statistics can be fully exploited. Furthermore, the purely experimental errors arising from the limited understanding of detector acceptances are uncorrelated among the experiments. Errors arising from limitations in theoretical precision, such as the calculation of the small-angle Bhabha cross-section, the t-channel contribution in the $\mathrm{e^+e^-}$ final state or pure QED corrections to the cross-section, are common to all experiments. They are discussed in detail in Section 5.

An overview of the experimental systematic errors is given in Table 3. The systematic error on the luminosity is common to cross-section measurements of all final states, but does not affect the measurements of A_fb.

2.2 Energy calibration

Precise knowledge of the centre-of-mass energy is essential for the determination of the mass and width of the Z resonance. The key features of the energy calibration procedure were the technique of resonant depolarisation and the careful monitoring of all relevant machine parameters [13]. The latter is important because beam energy calibrations with resonant depolarisation were possible only outside normal data taking, usually at the end of data taking in a particular fill of the accelerator, with fills typically lasting approximately 10 h. About 40% of the recorded off-peak luminosity was calibrated in this way in the 1993 scan and about 70% in the 1995 scan. For each experiment a value of the beam energy was provided every 15 minutes. These values were evaluated from the time evolutions of the relevant machine parameters. This required a model which took into account the fields in the LEP dipoles and in the corrector magnets, beam orbit positions, collision offsets at the interaction points and parameters of the radio-frequency system. In addition, environmental effects from leakage currents produced by trains in the Geneva area and the gravitational forces of the Moon and the Sun leading to small deformations of the accelerator geometry had to be considered. Errors on the centre-of-mass energy are largely dominated by the uncertainties in this model. The energy errors vary slightly among the interaction points, largely due to different configurations of the radio frequency cavities. The energy errors for different experiments and periods of data taking have large

	Aleph			Delphi		
	'93	'94	'95	'93	'94	'95
$\mathcal{L}^{\text{exp.}}$	0.067%	0.073%	0.080%	0.24%	0.09%	0.09%
σ_{had}	0.069%	0.072%	0.073%	0.10%	0.11%	0.10%
σ_{e}	0.15%	0.13%	0.15%	0.46%	0.52%	0.52%
σ_{μ}	0.11%	0.09%	0.11%	0.28%	0.26%	0.28%
σ_{τ}	0.26%	0.18%	0.25%	0.60%	0.60%	0.60%
A_{fb}^{e}	0.0006	0.0006	0.0006	0.0026	0.0021	0.0020
A_{fb}^{μ}	0.0005	0.0005	0.0005	0.0009	0.0005	0.0010
A_{fb}^{τ}	0.0009	0.0007	0.0009	0.0020	0.0020	0.0020

	L3			Opal		
	'93	'94	'95	'93	'94	'95
$\mathcal{L}^{\text{exp.}}$	0.086%	0.064%	0.068%	0.033%	0.033%	0.034%
σ_{had}	0.042%	0.041%	0.042%	0.073%	0.073%	0.085%
σ_{e}	0.24%	0.17%	0.28%	0.17%	0.14%	0.16%
σ_{μ}	0.32%	0.31%	0.40%	0.16%	0.10%	0.12%
σ_{τ}	0.68%	0.65%	0.76%	0.49%	0.42%	0.48%
A_{fb}^{e}	0.0025	0.0025	0.0025	0.001	0.001	0.001
A_{fb}^{μ}	0.0008	0.0008	0.0015	0.0007	0.0004	0.0009
A_{fb}^{τ}	0.0032	0.0032	0.0032	0.0012	0.0012	0.0012

Table 3: *Experimental systematic errors for the analysis of the Z line shape and lepton forward-backward asymmetries at the Z peak. None of the common errors discussed in Section 5 are included here.*

common parts, and therefore the use of a full correlation matrix is necessary. Assuming that all experiments contribute with the same weight allows all the LEP energy errors to be conveniently summarised in a single error matrix, common to all interaction points, as given in Table 4.

The energy of individual beam particles is usually not at the mean value considered above, but oscillates around the mean beam energy. Therefore observables are not measured at a sharp energy, E^0_{cm}, but instead their values are averaged over a range in energies $E^0_{cm} \pm \delta E_{cm}$. With the assumption of a Gaussian shape of the energy distribution, the total cross-sections receive a correction proportional to δE^2_{cm} and the second derivative of $\sigma(E_{cm})$ w.r.t. E_{cm}. At LEP I, typical values of the centre-of-mass energy spread are around 50 MeV. The effects of the correction lead to an increase of the cross-section at the peak of the Z resonance by 0.16% and a decrease of the width by about 5 MeV. The uncertainties on the energy spread, around ± 1 MeV in 1993–1995, constitute a negligible source of error common to all experiments.

In addition to the natural energy spread, changes in the mean beam energy due to

	‘93 p-2	‘93 p	‘93 p+2	‘94 p	‘95 p-2	‘95 p	‘95 p+2
‘93 p-2	3.42						
‘93 p	2.76	6.69					
‘93 p+2	2.59	2.64	2.95				
‘94 p	2.25	2.38	2.16	3.62			
‘95 p-2	1.29	1.14	1.23	1.23	1.78		
‘95 p	1.19	1.20	1.25	1.30	1.24	5.39	
‘95 p+2	1.20	1.15	1.33	1.24	1.22	1.34	1.68

Table 4: *Signed square root of covariance matrix elements, ($\mathcal{V}^E$), in* MeV*, from the determination of the centre-of-mass energies for the scan points in 1993–1995 [13]. Elements above the diagonal are left blank for simplicity. The errors for the earlier years may be found in References 10, 11.*

changes of machine parameters have a similar effect. Periods of data taking with a very similar centre-of-mass energy were combined into a single energy point in the experimental analyses by performing a luminosity-weighted average. The additional energy spread resulting from this was only around 10 MeV, which adds in quadrature to the natural energy spread of the accelerator.

3 Parametrisation of the differential cross-section

The differential cross-section for fermion pair production around the Z resonance consists of three s-channel contributions: from Z exchange, photon exchange and from the interference between photon and Z diagrams, $\sigma(s) = \sigma^{\mathrm{z}} + \sigma^{\gamma} + \sigma^{\mathrm{int}}$. This can be cast into a Born-type structure with complex-valued, s-dependent form factors describing the couplings of the Z and the photon to fermions. In the Z pole approximation, valid for $s \simeq m_{\mathrm{Z}}^2$, these are taken to be constants. Neglecting initial and final state photon radiation, final state gluon radiation and fermion masses, the electroweak kernel cross-section can thus be written as

$$
\begin{aligned}
\frac{2s}{\pi}\frac{1}{N_c^{\mathrm{f}}}\frac{d\sigma_{\mathrm{ew}}}{d\cos\theta}(\mathrm{e^+e^-}\to\mathrm{f\bar{f}}) \;=\;& \\
&\underbrace{\left|\alpha(m_{\mathrm{Z}})Q^{\mathrm{f}}\right|^2(1+\cos^2\theta)}_{\gamma} \\
&\underbrace{-8\,\mathrm{Re}\left\{\alpha^*(m_{\mathrm{Z}})Q^{\mathrm{f}}\chi(s)\left[\mathcal{G}_V^{\mathrm{e}}\mathcal{G}_V^{\mathrm{f}}(1+\cos^2\theta)+2\mathcal{G}_A^{\mathrm{e}}\mathcal{G}_A^{\mathrm{f}}\cos\theta\right]\right\}}_{\gamma-\mathrm{Z}\ \ \text{interference}} \\
&\underbrace{\begin{array}{l}+16\,|\chi(s)|^2\left[(|\mathcal{G}_V^{\mathrm{e}}|^2+|\mathcal{G}_A^{\mathrm{e}}|^2)(|\mathcal{G}_V^{\mathrm{f}}|^2+|\mathcal{G}_A^{\mathrm{f}}|^2)(1+\cos^2\theta)\right. \\ \qquad\qquad\left.+8\,\mathrm{Re}\left\{\mathcal{G}_V^{\mathrm{e}}\mathcal{G}_A^{\mathrm{e}\,*}\right\}\mathrm{Re}\left\{\mathcal{G}_V^{\mathrm{f}}\mathcal{G}_A^{\mathrm{f}\,*}\right\}\cos\theta\right]\end{array}}_{\mathrm{Z}}
\end{aligned}
$$

with

$$\chi(s) = \frac{G_{\mathrm{F}} m_{\mathrm{Z}}^2}{8\pi\sqrt{2}} \frac{s}{s - m_{\mathrm{Z}}^2 + \mathrm{i}s\Gamma_{\mathrm{Z}}/m_{\mathrm{Z}}} \,.$$

Here $\alpha(m_{\mathrm{Z}})$ is the electromagnetic coupling constant at the scale of the Z mass, G_{F} is the Fermi constant, Q^{f} is the charge of the final state fermion, and the colour factor N_c^{f} is one for leptons (f=e, μ, τ) and three for quarks (f=u, d, s, c, b). The effective vector and axial vector couplings of fermions to the Z are denoted by $\mathcal{G}_V^{\mathrm{f}}$ and $\mathcal{G}_A^{\mathrm{f}}$. $\chi(s)$ is the propagator term characterized by a Breit-Wigner denominator with an s-dependent width.

In Bhabha final states, $\mathrm{e^+e^-} \to \mathrm{e^+e^-}$, the t-channel diagrams also contribute to the cross-sections, with a dominant contribution at large $\cos\theta$, *i.e.* in the forward direction. This contribution, as well as its interference with the s-channel, add to the pure s-channel cross-section for $\mathrm{e^+e^-} \to \mathrm{e^+e^-}$.

The $1 + \cos^2\theta$ terms in the above formula contribute to the total cross-section, whereas the terms multiplying $\cos\theta$ contribute only to the forward-backward asymmetries for an experimental acceptance symmetric in $\cos\theta$. The total cross-section is completely dominated by Z exchange. The $\gamma - \mathrm{Z}$ interference determines the energy dependence of the forward-backward asymmetries and dominates at off-peak energies, but the leading contribution from the real parts of the couplings vanishes at $\sqrt{s} = m_{\mathrm{Z}}$.

The inclusion of higher-order electroweak corrections is absorbed in $\mathcal{G}_A$ and $\mathcal{G}_V$ with small imaginary parts arising from electroweak form factors. The experimental measurements do not allow a simultaneous extraction of the real and imaginary parts, and therefore the effective couplings to be determined are defined as $g_A = \mathrm{Re}(\mathcal{G}_A)$ and $g_V = \mathrm{Re}(\mathcal{G}_V)$. The imaginary parts of $\mathcal{G}_A$ and $\mathcal{G}_V$ are explicitly accounted for in the fitting codes by setting them to their SM expectations. The effects of box diagrams are also taken into account at this level.

It is worth noting that the definitions of the mass and width with an s-dependent width term in the Breit-Wigner denominator are suggested by phase-space and the structure of the electroweak radiative corrections within the SM. They differ from other commonly used definitions, *e.g.* the real part of the pole position in the energy-squared plane, where the propagator term takes the functional form $\chi(s) \propto s/(s - \overline{\mathrm{m}}_{\mathrm{Z}}{}^2 + i\,\overline{\mathrm{m}}_{\mathrm{Z}}\overline{\Gamma}_{\mathrm{Z}})$. This gives an identical line shape if $\overline{\mathrm{m}}_{\mathrm{Z}}$ and $\overline{\Gamma}_{\mathrm{Z}}$ are related to m_{Z} and Γ_{Z} by the multiplicative factor $1/\sqrt{1 + \Gamma_{\mathrm{Z}}^2/m_{\mathrm{Z}}^2}$.

Photon radiation from the initial and final states, and their interference, is conveniently treated by convoluting the electroweak kernel cross-section, $\sigma_{ew}(s)$, with a QED radiator, $H_{\mathrm{QED}}^{\mathrm{tot}}$,

$$\sigma(s) = \int_{4\mathrm{m}_{\mathrm{f}}^2}^{1} dz\, H_{\mathrm{QED}}^{\mathrm{tot}}(z, s)\, \sigma_{ew}(zs) \,.$$

The difference between the forward and backward cross-sections entering into the determination of the forward-backward asymmetries, $\sigma_{\mathrm{F}} - \sigma_{\mathrm{B}}$, is treated in the same way using a radiator function $H_{\mathrm{QED}}^{\mathrm{FB}}$.

At the peak the QED de-convoluted total cross-section is 36 % larger than the measured one, and the peak position is shifted downwards by about 100 MeV. The estimated precision of this important correction is discussed in Section 5.4.1.

The partial Z decay widths are defined inclusively, *i. e.* they contain QED and QCD final state corrections and the contribution from the imaginary parts of the effective couplings,

$$\Gamma_{\mathrm{ff}} = N_c^{\mathrm{f}} \frac{G_{\mathrm{F}}\, m_{\mathrm{Z}}^3}{6\sqrt{2}\pi} \left(|\mathcal{G}_A^{\mathrm{f}}|^2 R_A^{\mathrm{f}} + |\mathcal{G}_V^{\mathrm{f}}|^2 R_V^{\mathrm{f}} \right) + \Delta_{ew/QCD}\,.$$

The radiator factors R_V^{f} and R_A^{f} take into account final state QED and QCD corrections as well as non-zero fermion masses; $\Delta_{ew/QCD}$ accounts for non-factorizable electroweak/QCD corrections. The inclusion of the imaginary parts of the couplings in the definition of the leptonic width, $\Gamma_{\ell\ell}$, leads to changes of 0.15 per-mil corresponding to only 15% of the LEP-combined experimental error on $\Gamma_{\ell\ell}$.

The total cross-section arising from the $\cos\theta$-symmetric Z production term can also be written in terms of the partial decay widths into the initial and final states, Γ_{ee} and Γ_{ff},

$$\sigma_{\mathrm{ff}}^{\mathrm{z}} = \sigma_{\mathrm{ff}}^{\mathrm{peak}} \frac{s\,\Gamma_{\mathrm{Z}}^2}{(s-m_{\mathrm{Z}}^2)^2 + s^2\Gamma_{\mathrm{Z}}^2/m_{\mathrm{Z}}^2},$$

$$\text{with } \sigma_{\mathrm{ff}}^{\mathrm{peak}} = \frac{1}{1+\delta_{\mathrm{QED}}}\sigma_{\mathrm{ff}}^0 \text{ and } \sigma_{\mathrm{ff}}^0 = \frac{12\,\pi}{m_{\mathrm{Z}}^2}\,\frac{\Gamma_{\mathrm{ee}}\Gamma_{\mathrm{ff}}}{\Gamma_{\mathrm{Z}}^2}\,.$$

The term $1/(1+\delta_{\mathrm{QED}})$ removes the final state QED correction included in the definition of Γ_{ee}.

No distinction of the flavours of produced quarks is made, and therefore the overall hadronic cross-section is measured, and is parameterised in terms of the hadronic width given by the sum over all quark final states,

$$\Gamma_{\mathrm{had}} = \sum_{\mathrm{q,\,q\neq t}} \Gamma_{\mathrm{q\overline{q}}}\,.$$

The decays of the Z to neutrinos are invisible in the detectors and give rise to the "invisible width", $\Gamma_{\mathrm{inv}} = N_\nu \Gamma_{\nu\nu}$, where N_ν is the number of light neutrino species. The invisible width can be determined from the measurements of the decay widths to all visible final states and the total width, which is given by the sum over all partial widths,

$$\Gamma_{\mathrm{Z}} = \Gamma_{\mathrm{ee}} + \Gamma_{\mu\mu} + \Gamma_{\tau\tau} + \Gamma_{\mathrm{had}} + \Gamma_{\mathrm{inv}}\,.$$

Because the measured cross-sections depend on products of the partial widths and also on the total width, the widths constitute a highly correlated parameter set. In order to reduce correlations among the fit parameters an experimentally-motivated set of six parameters is used to describe the total hadronic and leptonic cross-sections around the Z peak. These are

- the mass of the Z, m_{Z}, and the total width, Γ_{Z};

- the "hadronic pole cross-section",

$$\sigma_{\rm h}^0 \equiv \frac{12\pi}{m_{\rm Z}^2}\frac{\Gamma_{\rm ee}\Gamma_{\rm had}}{\Gamma_{\rm Z}^2}\,;$$

- the ratios

$$R_{\rm e} \equiv \Gamma_{\rm had}/\Gamma_{\rm ee}\,,\;\; R_{\mu} \equiv \Gamma_{\rm had}/\Gamma_{\mu\mu} \;\;\text{and}\;\; R_{\tau} \equiv \Gamma_{\rm had}/\Gamma_{\tau\tau}\,.$$

The leading contribution from γ-Z interference is proportional to the product of the vector couplings of the initial and final states and vanishes at $\sqrt{s} = m_{\rm Z}$, but becomes noticeable at off-peak energies and therefore affects the Z mass. Because a determination of all quark couplings is not possible, the γ-Z interference term in the hadronic final state is fixed to its SM value. The implications of this are discussed in Section 6.4.

Three additional parameters are needed to describe the leptonic forward-backward asymmetries for the processes $\rm e^+e^- \to e^+e^-$, $\rm e^+e^- \to \mu^+\mu^-$ and $\rm e^+e^- \to \tau^+\tau^-$. These are

- the "pole asymmetries", $A_{\rm FB}^{0,\rm e}$, $A_{\rm FB}^{0,\mu}$ and $A_{\rm FB}^{0,\tau}$.

Contrary to the partial widths, the pole asymmetries are defined purely in terms of the real parts of the effective Z couplings,

$$A_{\rm FB}^{0,\rm f} \equiv \frac{3}{4}\mathcal{A}_{\rm e}\mathcal{A}_{\rm f} \;\;\text{with}\;\; \mathcal{A}_{\rm f} = \frac{2\,g_V^{\rm f}/g_A^{\rm f}}{1+\left(g_V^{\rm f}\,/\,g_A^{\rm f}\right)^2}\,.$$

Due to the smallness of the leptonic forward-backward asymmetry at $\sqrt{s} = m_{\rm Z}$, QED corrections are as large as $A_{\rm FB}^{0,\ell}$ itself. The product of the axial vector couplings of the initial and final states determines the leading contribution of the γ-Z interference. This can be fixed with sufficient precision together with the vector couplings from simultaneous fits to the measured forward-backward asymmetries and cross-sections, requiring SM input only for the imaginary parts of the couplings.

Differences between the pseudo-observables and the QED de-convoluted observables at $\sqrt{s} = m_{\rm Z}$, arising from the interference between photon and Z diagrams and from the interplay between the real and imaginary parts of the photon and Z couplings, are small in the SM. $\sigma_{\rm ff}^{\rm peak}$, given in terms of the partial decay widths, agrees to better than 0.5 permil for both hadrons and leptons with the QED de-convoluted cross-sections without the photon exchange contribution at $\sqrt{s} = m_{\rm Z}$. This is only a small fraction of the LEP-combined experimental error. The difference between $A_{\rm FB}^{0,\ell}$ and the QED de-convoluted forward-backward asymmetry at the peak amounts to 0.0013, which is slightly larger than the LEP-combined error on $A_{\rm FB}^{0,\ell}$. It is therefore important to treat the imaginary parts correctly, however, the measurements are not sensitive to variations of the imaginary parts within their SM expectation.

The pseudo-observables introduced above cannot be considered as truly model-independent, because imaginary parts of the couplings as well as the γ-Z interference in the hadronic final state need to be fixed to their SM values. This leads to small "Standard Model remnants" in any attempted "model-independent" definition of the pseudo-observables. More details about the treatment of imaginary parts and SM remnants in the theory programs TOPAZ0 [14] and ZFITTER [15] are given in Reference 16. These computer codes make available the best current knowledge of QED and electroweak corrections within the minimal Standard Model and also provide a (quasi) model-independent approach based on the parametrisation of the cross-sections and forward-backward asymmetries, as described above.

4 Experimental results

The experimental results presented here have been slightly modified from those published by the experiments [1–4] in order to facilitate the combination procedure. The four dedicated sets of experimental results for the combination are summarised in Table 5.

All fits are based on versions 6.23 of ZFITTER and 4.4 of TOPAZ0. The published ALEPH results were derived using version 6.10 of ZFITTER, which did not yet contain the improved treatment of fermion pairs radiated from the initial state [17]. For the combination presented here, the ALEPH measurements were reanalysed using version 6.23 of ZFITTER.

Each experiment used the combined energy error matrix described above (Table 4). This makes a small difference at the level of 0.1 MeV on m_Z and Γ_Z and their errors only for L3, where uncertainties arising from the modelling of the radio frequency cavities are largest.

In the Bhabha final state, the s-t interference has a small dependence on the value of the Z mass. Although practically negligible for a single experiment, a consistent treatment becomes important for the combination. Despite some different choices in the publications of the individual analyses, all experiments evaluate the t, s-t channel correction at their own value of the Z mass for the results presented here. The resulting interdependencies between the Z mass and the parameters from the Bhabha final state are explicitely included in the error correlation coefficients between m_Z and R_e or $A_{FB}^{0,e}$.

The LEP experiments agreed to use a standard set of parameters for the calculation of the Standard Model remnants in the theory programs. The important parameters are the Z mass, $m_Z = 91.187$ GeV, the Fermi constant, $G_F = (1.16637 \pm 0.00001) \times 10^{-5}$ GeV^{-2} [18], the electromagnetic coupling constant, $\alpha^{(5)}(m_Z) = 1/128.877 \pm 0.090$ [3] [19], the strong coupling constant, $\alpha_s(m_Z) = 0.119 \pm 0.002$ [20], the top quark mass, $m_t = 174.3 \pm 5.1$ GeV [21], and finally the Higgs mass, m_H, which was fixed to 150 GeV. The dependence of the fit results arising from the uncertainties in these parameters is almost negligible, as is discussed in Section 5.4.3.

[3] $\alpha^{(5)}(m_Z)$ is the electromagnetic coupling constant at the scale of the Z mass for five quark flavours; the value and error given correspond to a correction due to hadronic vacuum polarisation of $\Delta\alpha_{had}^{(5)} = 0.02804 \pm 0.00065$.

		correlations								
		m_{Z}	Γ_{Z}	σ^0_{h}	R_{e}	R_{μ}	R_{τ}	$A^{0,\,\mathrm{e}}_{\mathrm{FB}}$	$A^{0,\,\mu}_{\mathrm{FB}}$	$A^{0,\,\tau}_{\mathrm{FB}}$
χ^2/N_{df}	= 169/176					Aleph				
m_{Z} [GeV]	91.1891 ± 0.0031	1.00								
Γ_{Z} [GeV]	2.4959 ± 0.0043	.038	1.00							
σ^0_{h} [nb]	41.558 ± 0.057	−.091	−.383	1.00						
R_{e}	20.690 ± 0.075	.102	.004	.134	1.00					
R_{μ}	20.801 ± 0.056	−.003	.012	.167	.083	1.00				
R_{τ}	20.708 ± 0.062	−.003	.004	.152	.067	.093	1.00			
$A^{0,\,\mathrm{e}}_{\mathrm{FB}}$	0.0184 ± 0.0034	−.047	.000	−.003	−.388	.000	.000	1.00		
$A^{0,\,\mu}_{\mathrm{FB}}$	0.0172 ± 0.0024	.072	.002	.002	.019	.013	.000	−.008	1.00	
$A^{0,\,\tau}_{\mathrm{FB}}$	0.0170 ± 0.0028	.061	.002	.002	.017	.000	.011	−.007	.016	1.00
χ^2/N_{df}	= 177/168					Delphi				
m_{Z} [GeV]	91.1864 ± 0.0028	1.00								
Γ_{Z} [GeV]	2.4876 ± 0.0041	.047	1.00							
σ^0_{h} [nb]	41.578 ± 0.069	−.070	−.270	1.00						
R_{e}	20.88 ± 0.12	.063	.000	.120	1.00					
R_{μ}	20.650 ± 0.076	−.003	−.007	.191	.054	1.00				
R_{τ}	20.84 ± 0.13	.001	−.001	.113	.033	.051	1.00			
$A^{0,\,\mathrm{e}}_{\mathrm{FB}}$	0.0171 ± 0.0049	.057	.001	−.006	−.106	.000	−.001	1.00		
$A^{0,\,\mu}_{\mathrm{FB}}$	0.0165 ± 0.0025	.064	.006	−.002	.025	.008	.000	−.016	1.00	
$A^{0,\,\tau}_{\mathrm{FB}}$	0.0241 ± 0.0037	.043	.003	−.002	.015	.000	.012	−.015	.014	1.00
χ^2/N_{df}	= 158/166					L3				
m_{Z} [GeV]	91.1897 ± 0.0030	1.00								
Γ_{Z} [GeV]	2.5025 ± 0.0041	.065	1.00							
σ^0_{h} [nb]	41.535 ± 0.054	.009	−.343	1.00						
R_{e}	20.815 ± 0.089	.108	−.007	.075	1.00					
R_{μ}	20.861 ± 0.097	−.001	.002	.077	.030	1.00				
R_{τ}	20.79 ± 0.13	.002	.005	.053	.024	.020	1.00			
$A^{0,\,\mathrm{e}}_{\mathrm{FB}}$	0.0107 ± 0.0058	−.045	.055	−.006	−.146	−.001	−.003	1.00		
$A^{0,\,\mu}_{\mathrm{FB}}$	0.0188 ± 0.0033	.052	.004	.005	.017	.005	.000	.011	1.00	
$A^{0,\,\tau}_{\mathrm{FB}}$	0.0260 ± 0.0047	.034	.004	.003	.012	.000	.007	−.008	.006	1.00
χ^2/N_{df}	= 155/194					Opal				
m_{Z} [GeV]	91.1858 ± 0.0030	1.00								
Γ_{Z} [GeV]	2.4948 ± 0.0041	.049	1.00							
σ^0_{h} [nb]	41.501 ± 0.055	.031	−.352	1.00						
R_{e}	20.901 ± 0.084	.108	.011	.155	1.00					
R_{μ}	20.811 ± 0.058	.001	.020	.222	.093	1.00				
R_{τ}	20.832 ± 0.091	.001	.013	.137	.039	.051	1.00			
$A^{0,\,\mathrm{e}}_{\mathrm{FB}}$	0.0089 ± 0.0045	−.053	−.005	.011	−.222	−.001	.005	1.00		
$A^{0,\,\mu}_{\mathrm{FB}}$	0.0159 ± 0.0023	.077	−.002	.011	.031	.018	.004	−.012	1.00	
$A^{0,\,\tau}_{\mathrm{FB}}$	0.0145 ± 0.0030	.059	−.003	.003	.015	−.010	.007	−.010	.013	1.00

Table 5: *Results on Z parameters and their correlation coefficients.*

5 Common uncertainties

Important common errors among the results from all LEP experiments arise from several sources. These are the calibration of the beam energy, the theoretical error on the calculation of the small-angle Bhabha cross-section used as the normalisation reaction for all cross-section measurements, the theoretical uncertainties in the t-channel and s-t interference contribution to the differential large-angle Bhabha cross-section, the theoretical uncertainties in the calculations of QED radiative effects and, finally, from small uncertainties in the parametrisation of the electroweak cross-section near the Z resonance in terms of the set of pseudo-observables the four collaborations agreed upon. These common errors are quantified in the following sub-sections and are used in the combination.

Other sources of common errors may arise from the use of common Monte Carlo generators and detector simulation programs. However, each group uses its own tuning procedures and event selections which best suit their detector, and therefore the related errors are treated as uncorrelated among the experiments.

5.1 Common energy uncertainties

For the purpose of combining the experimental results at the parameter level, the errors on the centre-of-mass energy of each individual cross-section or asymmetry measurement, as given in Table 4, need to be transformed into errors on the extracted pseudo-observables. The first step is to scale the energy errors by factors of $1 \pm \epsilon$, while maintaining the experimental errors fixed. Typical values of ϵ used are between 5 % and 20 %. Performing the standard fits with these scaled errors generates two pseudo-observable covariance matrices, $V_{\pm}$, from which the covariance matrix due to energy errors, V_E, can be separated from the other errors, V_{exp}, using the relation $(V_{\pm}) = (1 \pm \epsilon)^2 (V_E) + (V_{\mathrm{exp}})$. The validity of this procedure was verified using a data set restricted to the hadronic cross-section measurements of the years 1993–1995, which were combined both at the cross-section level and at the parameter level.

Table 15 and 16 in the appendix show the energy errors on the pseudo-observables extracted from the individual experimental data sets. The estimated energy errors differ slightly depending on which experimental data set is used to derive them. Combinations may be attempted based on each of them, or on the average. The central values and errors of each of the averaged parameters agree well to within 5 % of the error on that average. It is therefore most appropriate to take the average of the error estimates over the experiments as the common energy errors, which are shown in Table 6.

5.2 Common t-channel uncertainties

The t-channel and s-t interference contributions are calculated in the Standard Model using the program ALIBABA [22]. The s-t interference contribution to the t-channel correction in Bhabha final states depends on the value of the Z mass. For the purpose of this combination, all experiments parametrise the t and s-t contributions as a function of

	m_Z	Γ_Z	σ_h^0	R_e
m_Z [GeV]	0.0017			
Γ_Z [GeV]	−0.0006	0.0012		
σ_h^0 [nb]	−0.0018	−0.0027	0.011	
R_e	0.0017	−0.0014	0.0073	0.013

	$A_{FB}^{0,e}$	$A_{FB}^{0,\mu}$	$A_{FB}^{0,\tau}$
$A_{FB}^{0,e}$	0.0004		
$A_{FB}^{0,\mu}$	−0.0003	0.0003	
$A_{FB}^{0,\tau}$	−0.0003	0.0003	0.0003

Table 6: *Common energy errors for nine-parameter fits. Values are given as the signed square root of the covariance matrix elements in the same units as in Table 5; elements above the diagonal have been omitted for simplicity. The anti-correlation between electron and muon or tau asymmetries arises from the different energy dependence of the electron asymmetry due to the t-channel contribution.*

m_Z. This allows the t, s-t correction to follow the determination of m_Z in the fits, which results in a correlation between m_Z and R_e or $A_{FB}^{0,e}$. The change in correlation coefficients introduced by explicitly taking into account the m_Z dependence of the t channel in the fits is about $+10\,\%$ for the m_Z-R_e correlation and $-10\,\%$ for the m_Z-$A_{FB}^{0,e}$ one. These correlation coefficients take the changes in R_e and $A_{FB}^{0,e}$ properly into account when m_Z takes its average value in the combination of the four experiments.

The theoretical uncertainty on the t-channel correction is discussed in detail in Reference 23. The size of the uncertainty is typically 1.1 pb for the forward cross-section and 0.3 pb for the backward cross-section and depends slightly on the acceptance cuts [24]. All collaborations incorporate the theory uncertainty as an additional error on the electron pair cross-section and asymmetry. In order to evaluate the common error from this source, each collaboration performed two fits, with and without the theory error, and the quadratic differences of the covariance matrix elements for R_e and $A_{FB}^{0,e}$ are taken as an estimate of the common error. The unknown error correlation between energy points below and above the peak is included in the error estimates by adding in quadrature the observed shifts in mean values of R_e and $A_{FB}^{0,e}$ when varying this correlation between -1 and $+1$. The t, s-t related errors estimated by individual experiments are summarised in Table 17 in the appendix. Since these are all very similar, the average shown in Table 7 is taken as the common error matrix.

	R_e	$A_{FB}^{0,e}$
R_e	0.024	
$A_{FB}^{0,e}$	−0.0054	0.0014

Table 7: *Common errors arising from the t-channel and s-t interference contributions to the e^+e^- final states, given as the signed square root of the covariance matrix elements.*

5.3 Common luminosity uncertainties

The four collaborations use similar techniques to measure the luminosity of their data samples by counting the number of small-angle Bhabha scattered electrons. The experimental details of the four measurements differ sufficiently that no correlation is believed to exist in the experimental component of the luminosity errors. All four collaborations, however, use BHLUMI 4.04 [25], the best available Monte Carlo generator for small-angle Bhabha scattering, to calculate the acceptance of their luminosity counters. Therefore significant correlations exist in the errors assigned to the scale of the measured cross-sections due to the uncertainty in this common theoretical calculation.

This uncertainty is estimated to be 0.061 % [26] without applying a correction for the production of light fermion pairs, which is not calculated in BHLUMI, and enters as a contribution to the estimated error. A recent calculation of the contribution of light pairs [27] has allowed OPAL to explicitly correct for light pairs and reduce its theoretical luminosity uncertainty to 0.054 %. This is taken as common with the errors of the other three experiments, who between themselves share a mutual common error of 0.061 %.

These errors almost exclusively affect the hadronic pole cross-section, and contribute about half its total error after combination. The common luminosity error also introduces a small contribution to the covariance matrix element between Γ_Z and σ_h^0. This was neglected in the common error tables given above, as it had no noticeable effect on the combined result.

5.4 Common theory uncertainties

An additional class of common theoretical errors arises from the approximations and special choices made in the fitting codes. These comprise contributions from QED radiative corrections, including initial-state pair radiation, and the parametrisation of the differential cross-section around the Z resonance in terms of pseudo-observables defined precisely at the peak and for pure Z exchange only. In order to estimate the uncertainties from the parametrisation of the electroweak cross-sections near the Z resonance the two most advanced calculational tools, ZFITTER [15] and TOPAZ0 [14], were compared. In addition, there are "parametric uncertainties" arising from parameters of the SM that are needed to fix the SM remnants.

5.4.1 QED uncertainties

The effects of initial state photon and fermion pair radiation lead to the large corrections in the vicinity of the Z resonance illustrated in Figure 1, and therefore play a central role in the extraction of the pseudo-observables from the measured cross-sections and asymmetries. Such large radiative effects have to be seen in contrast to the experimental precision, which is below the per-mil level in the case of the hadronic cross-section.

The most up-to-date evaluations of photonic corrections include the leading contributions up to $\mathcal{O}(\alpha^3)$. Two different schemes are available to estimate the remaining uncertainties:

1. KF: $\mathcal{O}(...\alpha^2 L^2, \alpha^2 L, \alpha^2 L^0)$ calculations [28] including the exponentiation scheme of Kuraev-Fadin [29] with $\mathcal{O}(\alpha^3 L^3)$ [30]. [4)]

2. YFS: the 2^{nd} order inclusive exponentiation scheme of Reference 31, 32, based on the YFS approach [33]. Third order terms are known and have only a small effect [34].

Differences between these schemes, which are both implemented in ZFITTER, TOPAZ0 and MIZA [35], and uncertainties due to missing higher order corrections [34], amount to at most ± 0.1 MeV on m_{Z} and Γ_{Z}, and $\pm 0.01\,\%$ on σ_{h}^0.

The influence of the interference between initial and final state radiation on the extracted parameters has also been studied recently [36], and uncertainties on m_{Z} of at most ± 0.1MeV from this source are expected for the experimental results given with only a small cut on s', the effective squared centre-of-mass energy after photon radiation from the initial state. The uncertainties due to the extrapolation of the leptonic s-channel cross-sections to full angular acceptance and from large to small s' are different among the experiments and are believed to be largely uncorrelated.

QED related uncertainties are dominated by the radiation of fermion pairs from the initial state. Starting from the full second order pair radiator [28, 37], a simultaneous exponentiation scheme for radiated photons and pairs was proposed in Reference 38. A third-order pair radiator was calculated recently [17] and compared with the other existing schemes, which are all available in the latest version of ZFITTER. Independent implementations of some schemes exist in TOPAZ0 and in MIZA. The largest uncertainty arises from the contribution of hadronic pairs. The maximum differences are 0.3 MeV on m_{Z}, 0.2 MeV on Γ_{Z} and $0.015\,\%$ on σ_{h}^0.

In summary, comparing the different options for photonic and fermion pair radiation leads to error estimates of ± 0.3 MeV on m_{Z} and ± 0.2 MeV on Γ_{Z}. The observed differences in σ_{h}^0 are slightly smaller than the error estimate of $\pm 0.02\,\%$ in Reference 34, which is therefore taken as the error for QED uncertainties.

5.4.2 Parametrisation of line shape and asymmetries

In a recent detailed comparison of TOPAZ0 and ZFITTER [16], cross-sections from Standard Model calculations and from the model-independent parametrisation were considered. Uncertainties on the pseudo-observables arise from differing choices in the parametrisation of the electroweak cross-sections near the Z resonance. In order to determine these TOPAZ0-ZFITTER differences, each of the two codes have been used. For practical reasons, cross-sections and forward-backward asymmetries were calculated with TOPAZ0 and then fitted with ZFITTER. Errors were assigned to the calculated cross-sections and forward-backward asymmetries which reflected the integrated luminosity taken at each energy, thus ensuring that each energy point entered with the appropriate weight.

The dominant part of the small differences between the two codes results from details of the implementation of the cross-section parametrisation in terms of the pseudo-observables.

[4)] Third-order terms for the KF scheme had also been calculated earlier [31].

Δm_Z [GeV]	$\Delta\Gamma_Z$ [GeV]	$\Delta\sigma_h^0$ [nb]	ΔR_ℓ	$\Delta A_{FB}^{0,\ell}$
0.0001	0.0001	0.001	0.004	0.0001

Table 8: *Differences in fit results obtained with TOPAZ0 and ZFITTER, taken as common systematic errors.*

This is particularly visible for the off-peak points, where the assignment of higher-order corrections to the Z resonance or to the SM remnants is not in all cases unambiguous. The size of the differences also depends on the particular values of the pseudo-observables, since these do not neccessarily respect the exact SM relations. Slightly different choices are made in the two codes if the SM relations between the pseudo-observables are not fulfilled. Finally, variations of factorisation schemes and other options in the electroweak calculations may affect the fit results through the SM remnants, but were found to have a negligible effect.

In Table 8 differences between TOPAZ0 and ZFITTER are shown, which are taken as common systematic errors. They were evaluated around the set of pseudo-observables representing the average of the four experiments, where the cross-sections and asymmetries were calculated for full acceptance with only a cut on $s' > 0.01\,s$. The only important systematic error of this kind is the one on R_ℓ, which amounts to 15 % of the combined error.

Putting all sources together, overall theoretical errors as listed in Table 9 are obtained, and these are used in the combination.

	m_Z	Γ_Z	σ_h^0	R_e	R_μ	R_τ	$A_{FB}^{0,e}$	$A_{FB}^{0,\mu}$	$A_{FB}^{0,\tau}$
m_Z[GeV]	0.0003								
Γ_Z[GeV]		0.0002							
σ_h^0[nb]			0.008						
R_e				0.004					
R_μ				0.004	0.004				
R_τ				0.004	0.004	0.004			
$A_{FB}^{0,e}$							0.0001		
$A_{FB}^{0,\mu}$							0.0001	0.0001	
$A_{FB}^{0,\tau}$							0.0001	0.0001	0.0001

Table 9: *Theoretical errors from fit programs, i.e. photon and fermion-pair radiation and model-independent parametrisation, given as the signed square root of the covariance matrix elements.*

5.4.3 Parametric uncertainties

Through the SM remnants the fit results depend slightly on the values of some SM parameters. Varying these within their present experimental errors, or between 100 GeV and 1000 GeV in case of the Higgs boson mass, leads to observable effects only on the Z mass, which is affected through the γ-Z interference term. The dominant dependence is on m_{H}, followed by $\alpha^{(5)}(m_{\mathrm{Z}})$.

The effect on m_{Z} from a variation of $1/\alpha^{(5)}(m_{\mathrm{Z}})$ by its error of ± 0.090 is ∓ 0.05 MeV, which is negligibly small compared to the systematic error on m_{Z} arising from other QED-related uncertainties (see Table 9). The change in m_{Z} due to m_{H} amounts to $+0.23$ MeV per unit change in $\log_{10}(m_{\mathrm{H}}/\mathrm{GeV})$. Note that this is small compared to the total error on m_{Z} of ± 2.1 MeV and is not considered as an error, but rather as a correction to be applied once the Higgs boson mass is known. The consequences of a completely model-independent treatment of the γ-Z interference in the hadronic channel are discussed in Section 6.4.

6 Combination of results

The combination of results on the Z parameters is based on the four sets of results on the nine parameters m_{Z}, Γ_{Z}, σ^0_{h}, R_{e}, R_μ, R_τ, $A^{0,\mathrm{e}}_{\mathrm{FB}}$, $A^{0,\mu}_{\mathrm{FB}}$ and $A^{0,\tau}_{\mathrm{FB}}$ and the common errors given in the previous chapter.

For this purpose it is necessary to construct the full $(4\times 9)\times(4\times 9)$ covariance matrix of the errors. The four diagonal 9×9 matrices consist of the four error matrices specified by each experiment (Table 5). The 9×9 common error matrices build the off-diagonal elements. Some theoretical uncertainties must also be added to the diagonal matrices, since they are not contained in the individual experimental matrices.

A symbolic representation of this matrix is shown in Table 10 . Each table element represents a 9×9 matrix; $(\mathcal{C}_{exp})$ for exp = A, D, L and O are the covariance matrices of the experiments (Table 5), and $(\mathcal{C}_c) = (\mathcal{C}_E) + (\mathcal{C}_\mathcal{L}) + (\mathcal{C}_t) + (\mathcal{C}_{\mathrm{QED,th}})$ is the matrix of common errors. Here (C_E) (Table 6) is the error matrix due to LEP energy uncertainties, $(C_\mathcal{L})$ (Section 5.3) arises from the theoretical error on the small-angle Bhabha cross-section calculations, (C_t) (Table 7) contains the errors from the t-channel treatment in the $\mathrm{e^+e^-}$ final state, and $(\mathcal{C}_{\mathrm{QED,th}})$ contains the errors from initial state photon and fermion pair radiation and from ambiguities in the model-independent parametrisation (Table 9). Since the latter errors were not included in the experimental error matrices, they were also added to the block matrices in the diagonal of Table 10 .

The combined parameter set and its covariance matrix are obtained from a χ^2 minimisation, with

$$\chi^2 = (\mathbf{X}-\mathbf{X_m})^T(\mathcal{C})^{-1}(\mathbf{X}-\mathbf{X_m}),$$

where $(\mathbf{X}-\mathbf{X_m})$ is the vector of residuals of the combined parameter set to the individual results.

Some checks of the combination procedure outlined above are described in the following subsections, and the combined results are given in the tables of Section 6.6.

$(\mathcal{C})$	Aleph	Delphi	L3	Opal
A	$(\mathcal{C}_A)+(\mathcal{C}_{\mathrm{QED,th}})$			
D	(C_c)	$(\mathcal{C}_D)+(\mathcal{C}_{\mathrm{QED,th}})$		
L	(C_c)	(C_c)	$(\mathcal{C}_L)+(\mathcal{C}_{\mathrm{QED,th}})$	
O	(C_c)	(C_c)	(C_c)	$(\mathcal{C}_O)+(\mathcal{C}_{\mathrm{QED,th}})$

Table 10: *Symbolic representation of the covariance matrix, $(\mathcal{C})$, used to combine the line shape and asymmetry results of the four experiments. Elements above the diagonal are the same as those below and are left blank for simplicity. The components of the matrix are explained in the text.*

6.1 Multiple-$\mathbf{m_Z}$ fits

In 1993 and 1995, the two years when Lep performed precision scans to measure the Z line shape, the experimental errors are very comparable, but the Lep energy was appreciably better understood in 1995 than in 1993. In determining the optimum value of m_Z, therefore, the four experiments combined should give more weight to the 1995 data than they each do in their independent determinations. To quantify this issue the measurements of each experiment were fitted to determine independent values of m_Z for the periods 1990–1992, 1993–94 and 1995. In this "eleven-parameter fit", each of the three mass values m_Z^{90-92}, m_Z^{93-94} and m_Z^{95} has its specific energy error reflecting the different systematic errors on the absolute energy scale of Lep. In the combination, the relative importance of energy related and independent experimental errors on the mass values is properly treated. The input and the common energy errors, estimated in the same way as for the nine parameters, are shown in Section A.3.

When the three values of m_Z are condensed into a single one, the effects of the time dependence of the precision in the energy calibration is taken into account. The difference of -0.2 MeV w.r.t. the m_Z value from the nine-parameter fits corresponds to 10 % of the combined error. All other parameters are identical to their values from the nine-parameter fit to within less than 5 % of the combined error. This result justifies using the standard combination based on the nine parameters. Tables 15 and 16 in the appendix show the energy errors on the pseudo-observables estimated from each individual experimental data set. The estimated energy errors differ slightly depending on which experimental data set is used to derive them. Combinations may be attempted based on each of them, or on the average. The central values and errors of each of the averaged parameters agree well within 5 % of the error on that average. It is therefore most appropriate to take the average of the error estimates over the experiments as the common energy errors, which are shown in Table 6.

The averages over the four experiments of the three values m_Z^{90-92}, m_Z^{93-94} and m_Z^{95} also provide a cross-check on the consistency of the energy calibration, which dominates the errors on m_Z in each of the periods considered. Using the energy errors of Table 19 allows the correlated and uncorrelated parts of the errors on the mass differences to be quantified.

This is shown in Figure 3. The differences between these values for the Z mass amount to $|m_Z^{90-92} - m_Z^{93-94}| = 31\,\%$, $|m_Z^{90-92} - m_Z^{95}| = 56\,\%$ and $|m_Z^{93-94} - m_Z^{95}| = 43\,\%$ of the uncorrelated error, *i. e.* the three Z mass values are well consistent.

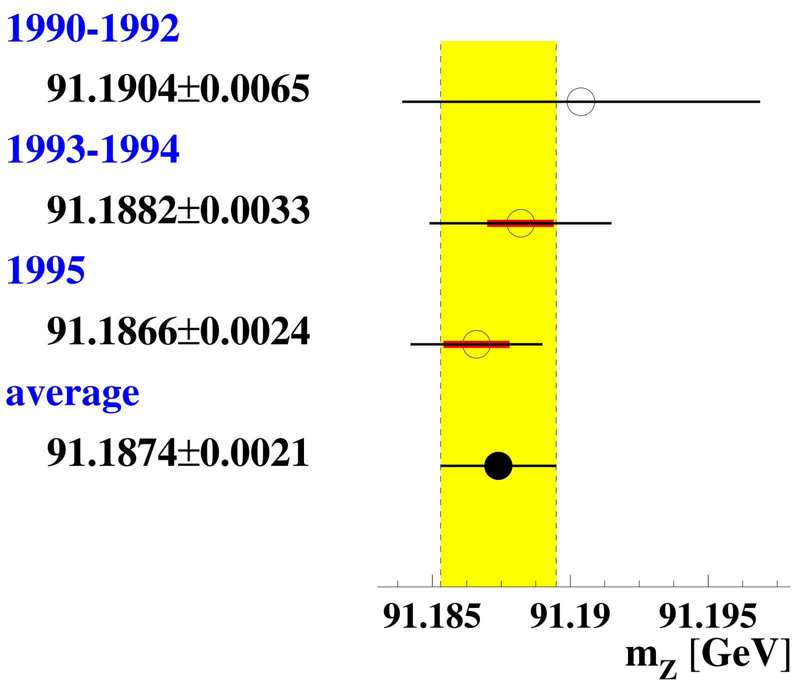

Figure 3: *m_Z in* GeV *for different periods of data taking, before 1993, 1993–1994 and 1995. The second, smaller error bar represents the correlated error component of 1.2* MeV *between m_Z^{93-94} and m_Z^{95}. m_Z^{90-92} is essentially uncorrelated with the other two.*

6.2 Fits with lepton universality

All experiments provide fits to their measured cross-sections and asymmetries with lepton universality imposed, *i. e.* R_e, R_μ and R_τ are replaced by R_ℓ and $A_{FB}^{0,e}$, $A_{FB}^{0,\mu}$ and $A_{FB}^{0,\tau}$ get replaced by $A_{FB}^{0,\ell}$ in the model-independent parametrisation of the differential cross-section. Here R_ℓ is defined for massless leptons. The individual experimental results and the correlation matrices are given in Table 18 in the appendix.

Comparing these five-parameter results with the nine-parameter results of Table 5, there is a noticeable change in m_Z of a few tenth of MeV in all experiments. This is a consequence of the dependence of the t-channel correction on m_Z, as discussed in Section 5.2. When R_e and $A_{FB}^{0,e}$ are replaced by the leptonic quantities R_ℓ and $A_{FB}^{0,\ell}$, their correlation with the

Z mass leads to a shift, which is driven by the (statistical) difference between R_{e} and R_ℓ and $A_{\mathrm{FB}}^{0,\mathrm{e}}$ and $A_{\mathrm{FB}}^{0,\ell}$. Similarly, replacing R_{e} and $A_{\mathrm{FB}}^{0,\mathrm{e}}$ from the values of a single experiment by the LEP average introduces a shift in m_{Z} in the presence of these particular correlation coefficients. Such shifts should become smaller when averaged over the four experiments. Indeed, the average of the shifts is only $-0.2\,\mathrm{MeV}$.

Another aspect of the five-parameter results concerns the role of the common t-channel uncertainty in the averages over the leptonic measurements to obtain R_ℓ and $A_{\mathrm{FB}}^{0,\ell}$. If the average over the leptonic measurements is performed by each experiment individually, the weight given to the electron channel is larger than for the case where the averages over individual lepton species are averaged at the end. In the latter procedure the weight of the electrons relative to the muon and tau final states is reduced due to the common t-channel error. Extracting the results with lepton universality from the nine parameters is therefore the appropriate method.

6.3 Shifts for halved experimental errors

When the average over the experiments is performed at the parameter level, information on the individual contribution of particular data points to the average is lost. Performing the average over the data points instead may therefore lead to changes of the relative importance of independent experimental errors w.r.t. the common errors. The examples of m_{Z} and the importance of the t-channel errors for R_ℓ, as discussed in the previous subsections, provide good illustrations of such effects. It was demonstrated that averaging the shifts in m_{Z} which each experiment observed when halving its experimental errors to simulate the generic "combined" experiment also reproduced the results of the full fit to the combined hadronic cross-section measurements.

While m_{Z} is properly treated by the eleven-parameter fits, other pseudo-observables may suffer from similar changes due to shifts of the weights. Changes in central values when halving the independent experimental errors in each experiment can be used as a monitoring tool for these parameters as well. The average of these changes over the four LEP experiments serves to control the differences between an average at the parameter level compared to a full cross-section average. Of course, this assumes that all measurements from individual experiments enter into the average with the same weight. The observed shifts are summarised in Table 11. The shift downwards in m_{Z} of $0.3\,\mathrm{MeV}$ corresponds to the slightly smaller shift of $0.2\,\mathrm{MeV}$ already seen in the multiple-m_{Z} fits.

Thus, the average changes in m_{Z}, σ_{h}^0, R_{e}, $A_{\mathrm{FB}}^{0,\mu}$ and $A_{\mathrm{FB}}^{0,\tau}$ amount to about $10\,\%$ of the combined errors, in all other cases they are even smaller.

This cross-check provides an estimate of the magnitude of the changes in the final results that would arise from a combination at the cross-section level. The averaging at the parameter level is equal to this within at most $10\,\%$ of the combined error.

	A	D	L	O	average	% of error
m_Z [GeV]	-0.0006	0.0000	-0.0004	-0.0001	-0.00028	13
Γ_Z [GeV]	-0.0002	$+0.0001$	-0.0004	0.0000	-0.00013	5
σ_h^0 [nb]	$+0.006$	0.000	$+0.008$	$+0.0036$	$+0.0037$	10
R_e	$+0.004$	$+0.017$	0.000	$+0.004$	$+0.0063$	13
R_μ	0.000	0.000	0.000	$+0.001$	0.0000	0
R_τ	0.000	0.000	-0.001	$+0.002$	$+0.0003$	1
$A_{FB}^{0,e}$	-0.0001	-0.0003	0.0000	-0.0000	-0.00011	5
$A_{FB}^{0,\mu}$	$+0.0002$	$+0.0003$	0.0000	$+0.0001$	$+0.00014$	11
$A_{FB}^{0,\tau}$	$+0.0002$	$+0.0003$	0.0000	$+0.0001$	$+0.00015$	9

Table 11: *Shifts in central values of the fitted pseudo-observables seen when halving the independent experimental errors, for individual experiments and average.*

6.4 Influence of the γ-Z interference term

In the nine-parameter analyses discussed here, the γ-Z interference terms in the differential cross-sections for leptons are expressed using the effective coupling constants and the electric charges of the electron, Q^e, and the final state fermion, Q^f (see equation for the differential cross-section in Section 3). For the hadronic final state, however, the γ-Z interference terms are fixed to the SM values, as individual quark flavours are not separated. Fits with a free interference term are possible in the S-Matrix scheme [39]. The OPAL collaboration also studied a different approach [4] based on an extension of the standard parameter set. In the S-Matrix approach the interference terms are considered as free and independent parameters. The hadronic interference term is described by the parameter j_{tot}^{had}, given in the SM by

$$j_{tot}^{had} = \frac{G_F m_Z^2}{\sqrt{2}\pi\alpha(m_Z)} Q^e g_V^e \times 3 \sum_q Q^q g_V^q \, .$$

Note that the running of α as well as final state QED and QCD corrections are also included in the definition of the S-Matrix parameters. The SM value of j_{tot}^{had} is 0.21 ± 0.01.

The dependence of the nine parameters on the hadronic γ-Z interference term is studied here by considering a set of ten parameters consisting of the standard nine parameters extended by the parameter j_{tot}^{had} from the S-Matrix approach. The γ-Z interference terms in the lepton channels are fixed by the leptonic Z couplings. As already observed in S-Matrix analyses of the LEP I data [3, 4], a large anti-correlation between m_Z and j_{tot}^{had} appears, leading to errors on m_Z enlarged by a factor of almost three. The studies show that the dependence of m_Z on j_{tot}^{had} is given by

$$\frac{dm_Z}{dj_{tot}^{had}} = -1.6\,\mathrm{MeV}/0.1 \, .$$

The changes in all other parameters are below 20 % of the errors in the combination for a change in j_{tot}^{had} of 0.1 .

Better experimental constraints on the hadronic interference term are obtained by including measurements of the hadronic total cross-section at centre-of-mass energies further away from the Z pole than just the off-peak energies at LEP I. Including the measurements of the TRISTAN collaborations TOPAZ [40] and VENUS [41] at $\sqrt{(s)}$=58 GeV, the error on $j_{\mathrm{tot}}^{\mathrm{had}}$ is reduced to ± 0.1, while its central value is in good agreement with the SM expectation. Measurements at centre-of-mass energies above the Z resonance at LEP II also provide constraints on $j_{\mathrm{tot}}^{\mathrm{had}}$, but in addition test modifications to the interference terms arising from the possible existence of a heavy Z' boson [42–45].

The available experimental constraints on $j_{\mathrm{tot}}^{\mathrm{had}}$ thus lead to uncertainties on m_{Z}, independent of SM assumptions in the hadronic channel, which are already smaller than its error. No additional error is assigned to the standard nine-parameter results from effects which might arise from a non-SM behaviour of the γ-Z interference.

6.5 Direct Standard Model fits to the measured cross-sections and forward-backwards asymmetries

Since an important use of the combined results presented here is to determine parameters of the SM and to make tests on its validity, it is crucial to verify that the parameter set we have chosen for the combination represents the four sets of experimental measurements from which they were extracted in a manner adequate to this purpose. When the set of pseudo-observables is used in the framework of the Standard Model, the role of m_{Z} changes from an independent parameter to that of a Lagrangian parameter of the theory. This imposes additional constraints which can be expected to shift the value of m_{Z}.

To check whether the nine parameters adequately describe the reaction to these constraints, each collaboration provided results from direct Standard Model fits to their cross-section and asymmetry data. The comparison of these results with those obtained by using the set of pseudo-observables as fit input is shown in Table 12. m_{H} and α_s were free parameters in these fits, while the additional inputs m_{t}=174.3$\pm$5.1 GeV and $\Delta\alpha_{\mathrm{had}}^{(5)} = 0.02804 \pm 0.00065$ (corresponding to $1/\alpha^{(5)}(m_{\mathrm{Z}}) = 128.877 \pm 0.090$) provided external constraints.

Most noticeably, significant shifts in m_{Z} are observed in some individual data sets, which cancel to almost zero in the average over the four experiments. One anticipated source of these shifts was already mentioned: the Z couplings defining the γ-Z interference term depend on m_{H}, which is allowed to move freely in the fit for SM parameters, but is fixed to 150 GeV in the model-independent fit for the extraction of the pseudo-observables. The approximate values of m_{H} preferred by the SM fit to the cross-sections and asymmetries are indicated in the second part of the table. Using the dependence of m_{Z} on the value of m_{H} given in Section 5.4.3, the differences in m_{Z} can be corrected to a common value of the Higgs mass of m_{H}=150 GeV, as is shown in the last line of Table 12. Hence the net average difference in m_{Z} directly from the data or through the intermediary of the nine parameters is less than 0.1 MeV. Shifts in the other SM parameters, in the individual data sets as well as in the average, are all well under 5 % of the errors, and therefore also negligible.

	A	D	L	O	average	% of error
$\chi^2/N_{\rm df}$	174/180	184/172	168/170	161/198		
$\Delta m_{\rm Z}$ [MeV]	-0.7	$+0.5$	0.0	$+0.1$	-0.03	1
$\Delta m_{\rm t}$ [GeV]	0.0	0.0	0.0	0.0	0.0	<2
$\Delta\log_{10}(m_{\rm H}/{\rm GeV})$	-0.01	$+0.04$	$+0.02$	$+0.04$	$+0.02$	4
$\Delta\alpha_s$	0.0000	-0.0002	$+0.0002$	$+0.0002$	$+0.0001$	4
$\Delta(\Delta\alpha^{(5)}_{\rm had})$	$+0.00002$	-0.00004	0.00000	-0.00004	-0.00002	2
fit value of $m_{\rm H}$ [GeV]	40.	10.	35.	390.		
$\Delta m_{\rm Z}$ [MeV] corrected to $m_{\rm H}$=150 GeV	-0.6	$+0.7$	$+0.1$	0.0	$+0.05$	2

Table 12: *Shifts in SM parameters, from direct SM fit to the cross-sections and forward-backward asymmetries w.r.t. fits to the nine-parameter results. The numbers in the lowest part of the table give the shifts in $m_{\rm Z}$ if the results from the first line are corrected to a common value of the Higgs mass of 150* GeV*.*

The conclusion of this study is that SM parameters extracted from the pseudo-observables are almost identical to the ones that would be extracted from the combined cross-sections and asymmetries. Within the SM the combined set of pseudo-observables provides a description of the measurements of the Z parameters that is equivalent to the full set of cross-sections and asymmetries. This is also true for any theory beyond the SM which leads to corrections that are absorbed in the pseudo-observables. An exception to this are those theories with an additional Z′-bosons which have significant modifications of the γ-Z interference term. (See the discussion in Section 6.4.)

6.6 Combined results

The result of the combination of the four sets of nine pseudo-observables of Table 5, including the experimental and common error matrices shown in Table 10, is given in Table 13. The value of the Higgs boson mass was assumed to be 150 GeV and is relevant only for the value of $m_{\rm Z}$, which changes by +0.23 MeV per unit change in $\log_{10}(m_{\rm H}/{\rm GeV})$. (See Section 5.4.3.)

The value of χ^2 per degree of freedom of the combination is 32.6/27 and corresponds to a probability of 21 % to find an agreement among the four sets of measurements which is worse than the one actually observed. The correlation matrix of the combined result shows significant correlations of $\sigma^0_{\rm h}$ with $\Gamma_{\rm Z}$ and $R_{\rm e}$, R_μ and R_τ and between $R_{\rm e}$ and $A^{0,{\rm e}}_{\rm FB}$.

A comparison of the leptonic quantites $R_{\rm e}$, R_μ and R_τ and of $A^{0,{\rm e}}_{\rm FB}$, $A^{0,\mu}_{\rm FB}$ and $A^{0,\tau}_{\rm FB}$ shows that they agree within errors. Note that R_τ is expected to be larger by 0.23 % because of τ mass effects. Figure 4 shows the corresponding 68 % level contours in the R_ℓ-$A^{0,\ell}_{\rm FB}$ plane.

Imposing the additional requirement of lepton universality in the combination leads to

without lepton universality		correlations								
$\chi^2/N_{\mathrm{df}} = 32.6/27$		m_{Z}	Γ_{Z}	σ^0_{h}	R_{e}	R_μ	R_τ	$A_{\mathrm{FB}}^{0,\,\mathrm{e}}$	$A_{\mathrm{FB}}^{0,\,\mu}$	$A_{\mathrm{FB}}^{0,\,\tau}$
m_{Z} [GeV]	91.1876 ± 0.0021	1.00								
Γ_{Z} [GeV]	2.4952 ± 0.0023	−.024	1.00							
σ^0_{h} [nb]	41.541 ± 0.037	−.044	−.297	1.00						
R_{e}	20.804 ± 0.050	.078	−.011	.105	1.00					
R_μ	20.785 ± 0.033	.000	.008	.131	.069	1.00				
R_τ	20.764 ± 0.045	.002	.006	.092	.046	.069	1.00			
$A_{\mathrm{FB}}^{0,\,\mathrm{e}}$	0.0145 ± 0.0025	−.014	.007	.001	−.371	.001	.003	1.00		
$A_{\mathrm{FB}}^{0,\,\mu}$	0.0169 ± 0.0013	.046	.002	.003	.020	.012	.001	−.024	1.00	
$A_{\mathrm{FB}}^{0,\,\tau}$	0.0188 ± 0.0017	.035	.001	.002	.013	−.003	.009	−.020	.046	1.00

with lepton universality						
$\chi^2/N_{\mathrm{df}} = 36.5/31$		m_{Z}	Γ_{Z}	σ^0_{h}	R_ℓ	$A_{\mathrm{FB}}^{0,\,\ell}$
m_{Z} [GeV]	91.1875 ± 0.0021	1.00				
Γ_{Z} [GeV]	2.4952 ± 0.0023	−.023	1.00			
σ^0_{h} [nb]	41.540 ± 0.037	−.045	−.297	1.00		
R_ℓ	20.767 ± 0.025	.033	.004	.183	1.00	
$A_{\mathrm{FB}}^{0,\,\ell}$	0.0171 ± 0.0010	.055	.003	.006	−.056	1.00

Table 13: *Result of the combination of the four sets of nine pseudo-observables from Table 5.*

the results shown in the second part of Table 13. Here R_ℓ is not a simple average over the three lepton species, but refers to Z decays into pairs of one massless charged lepton species. The value of χ^2/N_{df} of 36.5/31 for the combination of the four sets of nine pseudo-observables into the five parameters of Table 13 corresponds to a χ^2-probability of 23 %. The central ellipse in Figure 4 shows the 68 %-CL contour for the combined values of R_ℓ and $A_{\mathrm{FB}}^{0,\ell}$ determined from all three lepton species.

In principle, the average over the four experiments can also be performed at the level of the five parameter results of Section 6.2. When this is attempted, good agreement is seen with the results in the last line of Table 13, except for R_ℓ, where the difference amounts to 0.005 or 20 % of the total error. The origin of this shift is the common t-channel error, as discussed in Section 6.2 above.

6.7 Parameter Transformations

Additional pseudo-observables, more familiar than the experimentally motivated set of Table 13, can be obtained by parameter transformations. The partial Z decay widths are summarised in Table 14; it should be noted that these have larger correlations than the original set of results. If lepton universality is imposed, the value of Γ_{had} also changes and its error is reduced, because Γ_{ee} in the relation between the hadronic pole cross-section and the partial widths is replaced by the more precise value of $\Gamma_{\ell\ell}$. The invisible width, $\Gamma_{\mathrm{inv}} = \Gamma_{\mathrm{Z}} - \Gamma_{\mathrm{had}} - \Gamma_{\mathrm{ee}} - \Gamma_{\mu\mu} - \Gamma_{\tau\tau}$, is also shown in the table. The leptonic pole cross-section,

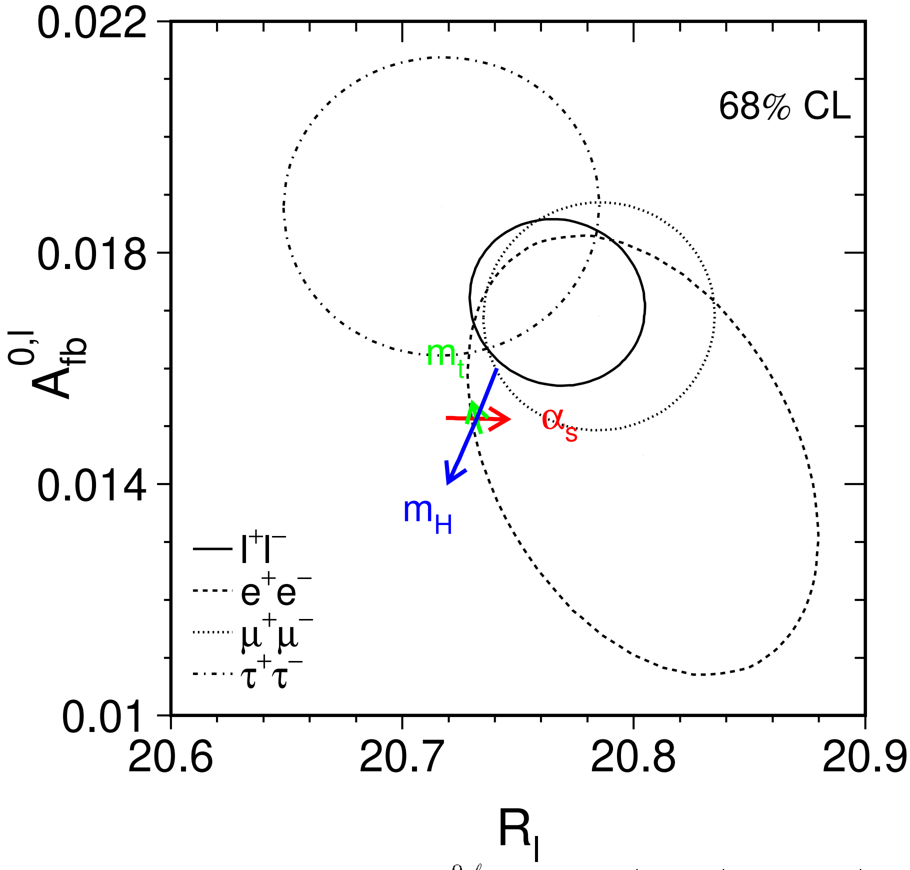

Figure 4: *Contour lines (68 % CL) in the* $R_\ell - \mathrm{A}_{\mathrm{FB}}^{0,\ell}$ *plane for* $\mathrm{e^+e^-}$, $\mu^+\mu^-$ *and* $\tau^+\tau^-$ *final states and for all leptons combined. For better comparison the results for the* τ *lepton are corrected to correspond to the massless case. The SM prediction for* m_Z*=91.1875* GeV*,* m_t*=174.3* GeV*,* m_H*=300* GeV *and* α_s*=0.119 is also shown. The lines with arrows correspond to the variation of the SM prediction when* m_t*,* m_H *and* α_s *are varied in the intervals* $m_\mathrm{t} = 174.3 \pm 5.1\,\mathrm{GeV}$*,* $m_\mathrm{H} = 300^{+700}_{-200}\,\mathrm{GeV}$*, and* $\alpha_s = 0.119 \pm 0.002$*, respectively. The arrows point in the direction of increasing values of* m_t*,* m_H *and* α_s*.*

σ_ℓ^o, defined as

$$\sigma_\ell^o \equiv \frac{12\pi}{m_\mathrm{Z}^2}\frac{\Gamma_{\ell\ell}^2}{\Gamma_\mathrm{Z}^2}\,,$$

in analogy to σ_h^0, is given in the last line of Table 14. Because QCD final state corrections appear quadratically in the denominator via Γ_Z, σ_ℓ^o has a higher sensitivity to α_s than σ_h^0 or R_ℓ, where the dependence on QCD corrections is only linear.

Assuming only standard particles, the invisible width is compatible with the SM hypothesis of decays into the three neutrino species, $\Gamma_\mathrm{inv} = 3\,\Gamma_{\nu\nu}$. The "number of neutrinos", N_ν, is calculated according to

$$\frac{\Gamma_\mathrm{inv}}{\Gamma_{\ell\ell}} = N_\nu \left(\frac{\Gamma_{\nu\nu}}{\Gamma_{\ell\ell}}\right)_\mathrm{SM}.$$

The Standard Model value for the ratio of the partial widths to neutrinos and to charged

without lepton universality		correlations			
Γ_{had} [MeV]	$1745.8\ \pm 2.7$	1.00			
Γ_{ee} [MeV]	83.92 ± 0.12	-0.29	1.00		
$\Gamma_{\mu\mu}$ [MeV]	83.99 ± 0.18	0.66	-0.20	1.00	
$\Gamma_{\tau\tau}$ [MeV]	84.08 ± 0.22	0.54	-0.17	0.39	1.00

with lepton universality				
Γ_{inv} [MeV]	$499.0\ \ \pm 1.5$	1.00		
Γ_{had} [MeV]	$1744.4\ \ \pm 2.0$	-0.29	1.00	
$\Gamma_{\ell\ell}$ [MeV]	83.984 ± 0.086	0.49	0.39	1.00
$\Gamma_{\mathrm{inv}}/\Gamma_{\ell\ell}$	5.942 ± 0.016			
σ^{o}_{ℓ} [nb]	2.0003 ± 0.0027			

Table 14: *Partial* Z *decay widths and correlation coefficients.*

leptons is 1.9912 ± 0.0012, where the uncertainty arises from variations of the top quark mass within its experimental error and of the Higgs mass within $100\,\mathrm{GeV} < m_{\mathrm{H}} < 1000\,\mathrm{GeV}$. With the measured value of $\Gamma_{\mathrm{inv}}\,/\,\Gamma_{\ell\ell} = 5.942 \pm 0.016$, the number of light neutrino species is determined to be

$$N_\nu = 2.9841 \pm 0.0083\ .$$

This may also be turned into a quantitative limit on extra, non-standard contributions to the invisible width, *i.e.* not originating from $\mathrm{Z} \to \nu\overline{\nu}$, by taking the difference between the value given in Table 14 and the Standard Model expectation of $(\Gamma_{\mathrm{inv}})_{\mathrm{SM}} = 501.7^{+0.1}_{-0.9}$ MeV. This gives $\Delta\Gamma_{\mathrm{inv}} = -2.7^{+1.7}_{-1.5}$ MeV, or expressed as a limit, $\Delta\Gamma_{\mathrm{inv}} < 2.0$ MeV @ 95% CL; here, the limit was conservatively calculated allowing only positive values of $\Gamma^{x}_{\mathrm{inv}}$.

The effective axial-vector and vector couplings of the Z to leptons, g^ℓ_A and g^ℓ_V, may be expressed in terms of the effective Veltman ρ parameter [46] and the effective weak mixing angle, $\sin^2\theta_{\mathrm{eff}}$, by

$$\begin{aligned} g^\ell_A &= \sqrt{\rho^{\mathrm{lept}}_{\mathrm{eff}}}\, I^\ell_3\ , \\ g^\ell_V &= \sqrt{\rho^{\mathrm{lept}}_{\mathrm{eff}}}\,(I^\ell_3 - 2Q^\ell \sin^2\theta^{\mathrm{lept}}_{\mathrm{eff}})\,, \end{aligned}$$

where $I^\ell_3 = -\frac{1}{2}$ is the weak iso-spin of charged leptons.

The leptonic pole asymmetry, $\mathrm{A}^{0,\ell}_{\mathrm{FB}}$, depends only on the ratio of the universal lepton couplings $g^\ell_V\,/\,g^\ell_A$, as is easily seen from its definition given in Section 3, and thus directly determines the effective weak mixing angle,

$$\sin^2\theta^{\mathrm{lept}}_{\mathrm{eff}} = \frac{1}{4}\left(1 - \frac{g^\ell_V}{g^\ell_A}\right)\ ,$$

if the sign of the ratio of couplings is chosen to be positive, in agreement with studies of the polarisation of τ leptons at LEP.

The leptonic width is almost entirely given by the parameter $\rho_{\mathrm{eff}}^{\mathrm{lept}}$, with a small contribution from the weak mixing angle entering through the vector couplings. A simultaneous fit of $\Gamma_{\ell\ell}$ and $A_{\mathrm{FB}}^{0,\ell}$ for $\rho_{\mathrm{eff}}^{\mathrm{lept}}$ and $\sin^2\theta_{\mathrm{eff}}^{\mathrm{lept}}$ results in

$$\begin{aligned} \rho_{\mathrm{eff}}^{\mathrm{lept}} &= 1.0048 \pm 0.0011\,, \\ \sin^2\theta_{\mathrm{eff}}^{\mathrm{lept}} &= 0.23099 \pm 0.00053\,, \end{aligned}$$

with an error correlation coefficient of 27 %.

Information on the effective ρ parameter contained in Γ_{inv} and Γ_{had} does not significantly improve on this result. From Γ_{inv}, the effective ρ parameter for neutrinos, $\rho_{\mathrm{eff}}^{\nu} = (2\,g^{\nu})^2$, is determined to be $\rho_{\mathrm{eff}}^{\nu} = 1.0027 \pm 0.0030$. The extraction of ρ from the hadronic width would require external constraints on the strong coupling constant and SM assumptions on flavour-dependent corrections.

The result on $\sin^2\theta_{\mathrm{eff}}^{\mathrm{lept}}$ derived here from the leptonic forward-backward asymmetries agrees well with the value recently published by SLD based on measurements of the left-right polarisation asymmetry of hadron production at the Z resonance [47]. The above value of $\rho_{\mathrm{eff}}^{\mathrm{lept}}$ is 4.4 standard deviations greater than its tree-level value of one, in good agreement with full SM calculations, and thus clearly shows the presence of genuine electroweak corrections.

7 Conclusion

The combination procedure adopted by the LEP electroweak working group for the four sets of pseudo-observables derived by the LEP experiments from the measured hadronic and leptonic cross-sections and the leptonic forward-backward asymmetries at centre-of-mass energies around the Z resonance has been described.

The combination procedure averages parameters extracted from the measurements of each individual experiment. This approximates a statistically optimal average that would be based on the measured cross-sections and forward-backward asymmetries to better than 10 % of the combined errors, *i. e.* the chosen set of parameters adequately represents the full set of measurements. The technical precision of the adopted combination procedure is around 5 % of the combined errors. Using each of the four sets of input parameters in the framework of the minimal Standard Model yields results which are on average identical, to within 5 % of the combined errors, to those obtained directly from Standard-Model fits to the measured cross-sections and asymmetries of each individual experiment.

Detailed studies of common systematic errors were performed. The dominant contribution of ± 1.7 MeV to the combined error on the Z mass arises from the calibration of the energy of the beams in LEP. The dominant contribution of ± 0.025 nb to the uncertainty on the hadronic cross-section at the pole of the Z resonance arises from the theoretical error on the small-angle Bhabha cross-section. The errors on all other parameters are dominated by independent experimental or statistical errors.

The combined LEP results on the mass and width of the Z, on the hadronic pole cross-section, on the ratio of the hadronic and leptonic partial width and on the pole forward-backward asymmetry are

$$\begin{aligned} m_{\mathrm{Z}} &= 91.1875 \pm 0.0021\,\mathrm{GeV}\,, \\ \Gamma_{\mathrm{Z}} &= 2.4952 \pm 0.0023\,\mathrm{GeV}\,, \\ \sigma^0_{\mathrm{h}} &= 41.540 \pm 0.037\,\mathrm{nb}\,, \\ R_\ell &= 20.767 \pm 0.025\,, \\ \mathrm{A}^{0,\ell}_{\mathrm{FB}} &= 0.0171 \pm 0.0010\,. \end{aligned}$$

Correlations are typically small ($\leq 5\,\%$), being significant only between σ^0_{h} and Γ_{Z} ($-30\,\%$) and between σ^0_{h} and R_ℓ ($18\,\%$). The full set of results and the error correlation matrices are shown in Table 13.

Acknowledgements

We wish to thank the CERN SL division for the excellent performance of the LEP collider, and the working group on energy calibration for providing a precise knowledge on the beam energies. We would also like to thank all our theorist colleagues who have contributed to the precision calculations of observables at the Z resonance, and the TOPAZ0 and ZFITTER teams who have incorporated these calculations and made them available to us.

A Appendix

A.1 Common errors estimated by individual experiments

		m_Z	Γ_Z	σ_h^0	R_e
ALEPH	m_Z [GeV]	0.0017			
	Γ_Z [GeV]	-0.0004	0.0012		
	σ_h^0 [nb]	-0.0028	-0.0024	0.011	
	R_e	0.0013	-0.0015	0.007	0.012
DELPHI	m_Z [GeV]	0.0016			
	Γ_Z [GeV]	-0.0005	0.0012		
	σ_h^0 [nb]	-0.0025	-0.0024	0.009	
	R_e	0.0014	0.0000	0.004	0.016
L3	m_Z [GeV]	0.0016			
	Γ_Z [GeV]	-0.0008	0.0013		
	σ_h^0 [nb]	-0.0009	-0.0030	0.011	
	R_e	0.0020	-0.0021	0.010	0.013
OPAL	m_Z [GeV]	0.0017			
	Γ_Z [GeV]	-0.0005	0.0012		
	σ_h^0 [nb]	-0.0011	-0.0028	0.011	
	R_e	0.0019	-0.0019	0.008	0.012

Table 15: *Common energy errors, from individual data sets for the nine-parameter fits. Values are given as the signed square root of the covariance matrix elements; elements above the diagonal have been omitted for simplicity.*

		$A_{FB}^{0,e}$	$A_{FB}^{0,\mu}$	$A_{FB}^{0,\tau}$
ALEPH	$A_{FB}^{0,e}$	0.0003		
	$A_{FB}^{0,\mu}$	−0.0003	0.0003	
	$A_{FB}^{0,\tau}$	−0.0003	0.0003	0.0003
DELPHI	$A_{FB}^{0,e}$	0.0004		
	$A_{FB}^{0,\mu}$	−0.0003	0.0003	
	$A_{FB}^{0,\tau}$	−0.0003	0.0003	0.0003
L3	$A_{FB}^{0,e}$	0.0003		
	$A_{FB}^{0,\mu}$	−0.0002	0.0003	
	$A_{FB}^{0,\tau}$	−0.0002	0.0002	0.0003
OPAL	$A_{FB}^{0,e}$	0.0004		
	$A_{FB}^{0,\mu}$	−0.0003	0.0003	
	$A_{FB}^{0,\tau}$	−0.0003	0.0003	0.0003

Table 16: *Common energy errors for forward-backward asymmetries, estimated from the data sets of individual experiments.*

		R_e	$A_{FB}^{0,e}$
ALEPH	R_e	0.025	
	$A_{FB}^{0,e}$	−0.0056	0.0013
DELPHI	R_e	0.025	
	$A_{FB}^{0,e}$	−0.0058	0.0016
L3	R_e	0.021	
	$A_{FB}^{0,e}$	−0.0046	0.0010
OPAL	R_e	0.025	
	$A_{FB}^{0,e}$	−0.0057	0.0015

Table 17: *Estimates of the t-channel errors of individual experiments.*

A.2 Results with lepton universality

		correlations				
		m_Z	Γ_Z	σ_h^0	R_ℓ	$A_{FB}^{0,\ell}$
χ^2/N_{df}	$= 172/180$	ALEPH				
m_Z [GeV]	91.1893 ± 0.0031	1.00				
Γ_Z [GeV]	2.4959 ± 0.0043	.038	1.00			
σ_h^0 [nb]	41.559 ± 0.057	−.092	−.383	1.00		
R_ℓ	20.729 ± 0.039	.033	.011	.246	1.00	
$A_{FB}^{0,\ell}$	0.0173 ± 0.0016	.071	.002	.001	−.076	1.00
χ^2/N_{df}	$= 183/172$	DELPHI				
m_Z [GeV]	91.1863 ± 0.0028	1.00				
Γ_Z [GeV]	2.4876 ± 0.0041	.046	1.00			
σ_h^0 [nb]	41.578 ± 0.069	−.070	−.270	1.00		
R_ℓ	20.730 ± 0.060	.028	−.006	.242	1.00	
$A_{FB}^{0,\ell}$	0.0187 ± 0.0019	.095	.006	−.005	.000	1.00
χ^2/N_{df}	$= 163/170$	L3				
m_Z [GeV]	91.1894 ± 0.0030	1.00				
Γ_Z [GeV]	2.5025 ± 0.0041	.068	1.00			
σ_h^0 [nb]	41.536 ± 0.055	.014	−.348	1.00		
R_ℓ	20.809 ± 0.060	.067	.020	.111	1.00	
$A_{FB}^{0,\ell}$	0.0192 ± 0.0024	.041	.020	.005	−.024	1.00
χ^2/N_{df}	$= 158/198$	OPAL				
m_Z [GeV]	91.1853 ± 0.0029	1.00				
Γ_Z [GeV]	2.4947 ± 0.0041	.051	1.00			
σ_h^0 [nb]	41.502 ± 0.055	.030	−.352	1.00		
R_ℓ	20.822 ± 0.044	.043	.024	.290	1.00	
$A_{FB}^{0,\ell}$	0.0145 ± 0.0017	.075	−.005	.013	−.017	1.00

Table 18: *Results on Z parameters and error correlation matrices by the four experiments with lepton universality imposed.*

A.3 Results from eleven-parameter fits

ALEPH

Γ_Z [GeV]	2.4957 ± 0.0043
σ_h^0 [nb]	41.559 ± 0.057
R_e	20.694 ± 0.075
R_μ	20.801 ± 0.056
R_τ	20.709 ± 0.062
$A_{FB}^{0,e}$	0.0184 ± 0.0034
$A_{FB}^{0,\mu}$	0.0173 ± 0.0025
$A_{FB}^{0,\tau}$	0.0171 ± 0.0028
m_Z^{90-92} [GeV]	91.1928 ± 0.0092
m_Z^{93-94} [GeV]	91.1926 ± 0.0046
m_Z^{95} [GeV]	91.1852 ± 0.0043

correlation matrix

1.000	−0.384	0.001	0.012	0.003	0.001	0.000	0.000	0.015	−0.011	0.055
−0.384	1.000	0.137	0.167	0.152	−0.004	0.003	0.003	−0.043	−0.037	−0.074
0.001	0.137	1.000	0.083	0.067	−0.389	0.020	0.017	0.063	0.063	0.036
0.012	0.167	0.083	1.000	0.093	0.000	0.014	0.000	0.003	−0.001	−0.004
0.003	0.152	0.067	0.093	1.000	0.000	0.000	0.012	0.001	−0.001	−0.004
0.001	−0.004	−0.389	0.000	0.000	1.000	−0.009	−0.008	−0.037	−0.036	−0.020
0.000	0.003	0.020	0.014	0.000	−0.009	1.000	0.018	0.056	0.063	0.022
0.000	0.003	0.017	0.000	0.012	−0.008	0.018	1.000	0.045	0.060	0.018
0.015	−0.043	0.063	0.003	0.001	−0.037	0.056	0.045	1.000	0.016	0.011
−0.011	−0.037	0.063	−0.001	−0.001	−0.036	0.063	0.060	0.016	1.000	0.093
0.055	−0.074	0.036	−0.004	−0.004	−0.020	0.022	0.018	0.011	0.093	1.000

DELPHI

Γ_Z [GeV]	2.4878 ± 0.0041
σ_h^0 [nb]	41.573 ± 0.069
R_e	20.88 ± 0.12
R_μ	20.650 ± 0.076
R_τ	20.84 ± 0.13
$A_{FB}^{0,e}$	0.0170 ± 0.0049
$A_{FB}^{0,\mu}$	0.0164 ± 0.0025
$A_{FB}^{0,\tau}$	0.0240 ± 0.0037
m_Z^{90-92} [GeV]	91.1883 ± 0.0084
m_Z^{93-94} [GeV]	91.1824 ± 0.0043
m_Z^{95} [GeV]	91.1894 ± 0.0038

correlation matrix

1.000	−0.271	−0.001	−0.007	−0.001	−0.001	0.005	0.003	0.002	0.012	0.062
−0.271	1.000	0.123	0.191	0.113	−0.003	0.002	0.001	−0.003	0.015	−0.066
−0.001	0.123	1.000	0.054	0.033	−0.105	0.027	0.016	0.055	0.044	0.029
−0.007	0.191	0.054	1.000	0.051	0.000	0.008	0.000	0.000	−0.002	−0.002
−0.001	0.113	0.033	0.051	1.000	−0.001	0.000	0.011	−0.001	−0.001	0.002
−0.001	−0.003	−0.105	0.000	−0.001	1.000	−0.014	−0.014	0.048	0.052	0.016
0.005	0.002	0.027	0.008	0.000	−0.014	1.000	0.015	0.057	0.053	0.021
0.003	0.001	0.016	0.000	0.011	−0.014	0.015	1.000	0.032	0.037	0.016
0.002	−0.003	0.055	0.000	−0.001	0.048	0.057	0.032	1.000	0.016	0.007
0.012	0.015	0.044	−0.002	−0.001	0.052	0.053	0.037	0.016	1.000	0.088
0.062	−0.066	0.029	−0.002	0.002	0.016	0.021	0.016	0.007	0.088	1.000

	L3
Γ_Z [GeV]	2.5024 ± 0.0041
σ_h^0 [nb]	41.540 ± 0.055
R_e	20.821 ± 0.089
R_μ	20.861 ± 0.097
R_τ	20.79 ± 0.13
$A_{FB}^{0,e}$	0.0106 ± 0.0058
$A_{FB}^{0,\mu}$	0.0190 ± 0.0033
$A_{FB}^{0,\tau}$	0.0261 ± 0.0047
m_Z^{90-92} [GeV]	91.1973 ± 0.0092
m_Z^{93-94} [GeV]	91.1912 ± 0.0047
m_Z^{95} [GeV]	91.1870 ± 0.0041

correlation matrix

1.000	−0.354	−0.001	−0.001	0.004	−0.002	−0.001	0.000	0.017	0.014	0.072
−0.354	1.000	0.081	0.078	0.055	0.011	0.011	0.007	0.087	0.022	−0.038
−0.001	0.081	1.000	0.030	0.024	−0.150	0.020	0.014	0.117	0.050	0.059
−0.001	0.078	0.030	1.000	0.020	−0.002	0.005	−0.000	0.002	−0.001	−0.001
0.004	0.055	0.024	0.020	1.000	−0.004	−0.000	0.009	0.002	0.001	0.002
−0.002	0.011	−0.150	−0.002	−0.004	1.000	0.011	−0.007	−0.044	−0.016	−0.037
−0.001	0.011	0.020	0.005	−0.000	0.011	1.000	0.007	0.051	0.047	0.010
0.000	0.007	0.014	−0.000	0.009	−0.007	0.007	1.000	0.025	0.034	0.008
0.017	0.087	0.117	0.002	0.002	−0.044	0.051	0.025	1.000	0.004	0.002
0.014	0.022	0.050	−0.001	0.001	−0.016	0.047	0.034	0.004	1.000	0.083
0.072	−0.038	0.059	−0.001	0.002	−0.037	0.010	0.008	0.002	0.083	1.000

OPAL	
Γ_Z [GeV]	2.4946 $\pm$ 0.0042
σ_h^0 [nb]	41.506 $\pm$ 0.057
R_e	20.903 $\pm$ 0.085
R_μ	20.812 $\pm$ 0.058
R_τ	20.833 $\pm$ 0.091
$A_{FB}^{0,e}$	0.0089 $\pm$ 0.0045
$A_{FB}^{0,\mu}$	0.0159 $\pm$ 0.0023
$A_{FB}^{0,\tau}$	0.0146 $\pm$ 0.0030
m_Z^{90-92} [GeV]	91.1851 $\pm$ 0.0091
m_Z^{93-94} [GeV]	91.1872 $\pm$ 0.0046
m_Z^{95} [GeV]	91.1849 $\pm$ 0.0039

correlation matrix

1.000	−0.369	0.001	0.019	0.012	−0.002	−0.009	−0.007	0.002	−0.065	0.107
−0.369	1.000	0.164	0.218	0.137	0.005	0.018	0.014	0.009	0.185	−0.100
0.001	0.164	1.000	0.090	0.042	−0.228	0.034	0.026	0.079	0.106	0.032
0.019	0.218	0.090	1.000	0.058	−0.002	0.012	−0.001	−0.007	0.005	0.000
0.012	0.137	0.042	0.058	1.000	0.000	0.000	0.016	−0.007	0.007	−0.001
−0.002	0.005	−0.228	−0.002	0.000	1.000	−0.017	−0.013	−0.040	−0.046	−0.021
−0.009	0.018	0.034	0.012	0.000	−0.017	1.000	0.019	0.062	0.073	0.024
−0.007	0.014	0.026	−0.001	0.016	−0.013	0.019	1.000	0.045	0.058	0.019
0.002	0.009	0.079	−0.007	−0.007	−0.040	0.062	0.045	1.000	0.021	0.006
−0.065	0.185	0.106	0.005	0.007	−0.046	0.073	0.058	0.021	1.000	0.093
0.107	−0.100	0.032	0.000	−0.001	−0.021	0.024	0.019	0.006	0.093	1.000

The common energy errors are shown in Table 19. The agreement of the energy-related errors for the eleven parameter results is acceptable among the experiments. Noticeable are the differences in the covariance matrix elements between the Z mass values and σ_h^0; they were traced back to slightly different strategies in choosing a value of m_Z in the different time periods for calculations involving the hadronic pole cross section.

		Γ_Z	σ_h^0	R_e	m_Z^{90-92}	m_Z^{93-94}	m_Z^{95}
ALEPH	m_Z^{90-92}	-0.0011	-0.002	0.0020	0.0058		
	m_Z^{93-94}	-0.0007	-0.003	0.0016	0.0006	0.0028	
	m_Z^{95}	0.0002	-0.002	0.0003	0.0003	0.0013	0.0015
DELPHI	m_Z^{90-92}	-0.0009	0.0014	0.0027	0.0053		
	m_Z^{93-94}	-0.0006	-0.0020	0.0014	0.0008	0.0027	
	m_Z^{95}	-0.0002	-0.0018	0.0007	0.0004	0.0012	0.0014
L3	m_Z^{90-92}	-0.0013	0.0045	0.0046	0.0050		
	m_Z^{93-94}	-0.0007	-0.0022	-0.0007	-0.0008	0.0028	
	m_Z^{95}	-0.0001	-0.0018	-0.0006	-0.0009	0.0012	0.0015
OPAL	m_Z^{90-92}	-0.0011	0.0025	0.0036	0.0058		
	m_Z^{93-94}	-0.0010	0.0034	0.0034	0.0006	0.0030	
	m_Z^{95}	0.0000	-0.0014	0.0013	-0.0003	0.0012	0.0015
average	m_Z^{90-92}	-0.0011	0.0016	0.0032	0.0055		
	m_Z^{93-94}	-0.0008	-0.0010	0.0014	0.0003	0.0028	
	m_Z^{95}	0.0000	-0.0018	-0.0004	-0.0001	0.0012	0.0015

Table 19: *Common energy errors for multiple-m_Z fit, from individual data sets and average. The matrix elements for Γ_Z, σ_h^0 and R_e and for the asymmetries are very similar to the nine-parameter case and can be taken from Table 15 and 16.*

References

[1] ALEPH Collaboration (D. Decamp *et al.*), Z. Phys. **C48** (1990) 365;
Z. Phys. **C53** (1992) 1;
ALEPH Collaboration (D. Buskulic *et al.*), Z. Phys. **C60** (1993) 71;
Z. Phys. **C62** (1994) 539;
ALEPH Collaboration (R. Barate *et al.*), Eur. Phys. J. **C14** (2000) 1.

[2] DELPHI Collaboration (P. Aarnio *et al.*), Nucl. Phys. **B367** (1991) 511;
DELPHI Collaboration (P. Abreu *et al.*), Nucl. Phys. **B417** (1994) 3;
Nucl. Phys. **B418** (1994) 403;
Eur. Phys. J. **C16** (2000) 371.

[3] L3 Collaboration (B. Adeva *et al.*), Z. Phys. **C51** (1991) 179;
L3 Collaboration (O. Adriani *et al.*), Phys. Rep. **236** (1993) 1;
L3 Collaboration (M. Acciarri *et al.*), Z. Phys. **C62** (1994) 551;
Eur. Phys. J. **C16** (2000) 1.

[4] OPAL Collaboration (G. Alexander *et al.*), Z. Phys. **C52** (1991) 175;
OPAL Collaboration (P.D. Acton *et al.*), Z. Phys. **C58** (1993) 219;
OPAL Collaboration (R. Akers *et al.*), Z. Phys. **C61** (1994) 19;
OPAL Collaboration (G. Abbiendi *et al.*), Eur. Phys. J. **C14** (2000) 373;
Precise Determination of the Z Resonance Parameters at LEP : Zedometry, CERN-EP-2000-148 (Nov. 2000), submitted to Eur. Phys. J. **C**.

[5] *Z Physics at LEP1*, CERN 89-08, ed. G. Altarelli *et al.*, Vol. 1–3 (1989) and references therein.

[6] ALEPH Collaboration (D. Decamp *et al.*), Nucl. Inst. Meth. **A294** (1990) 121;
ALEPH Collaboration (D. Buskulic *et al.*), Nucl. Inst. Meth. **A360** (1995) 481.

[7] DELPHI Collaboration (P. Aarnio *et al.*), Nucl. Inst. Meth. **A303** (1991) 233;
DELPHI Collaboration (P. Abreu *et al.*), Nucl. Inst. Meth. **A378** (1996) 57.

[8] L3 Collaboration (B. Adeva *et al.*), Nucl. Inst. Meth. **A289** (1990) 35;
L3 Collaboration (M. Acciarri *et al.*), Nucl. Inst. Meth. **A351** (1994) 300;
L3 Collaboration (M. Chemarin *et al.*), Nucl. Inst. Meth. **A349** (1994) 345;
L3 Collaboration (A. Adam *et al.*), Nucl. Inst. Meth. **A383** (1996) 342;
L3 Collaboration (I.C. Brock *et al.*), Nucl. Inst. Meth. **A381** (1996) 236.

[9] OPAL Collaboration (K. Ahmet *et al.*), Nucl. Inst. Meth. **A305** (1991) 275;
OPAL Collaboration (P. Allport *et al.*), Nucl. Inst. Meth. **A324** (1993) 34;
OPAL Collaboration (P. Allport *et al.*), Nucl. Inst. Meth. **A346** (1994) 476;
OPAL Collaboration (B.E. Anderson *et al.*), IEEE Trans. Nucl. Sci. **41** (1994) 845.

[10] The working group on LEP energy and the Collaborations ALEPH, DELPHI, L3 and OPAL, Phys. Lett. **B307** (1993) 187.

[11] Working group on LEP energy (L. Arnaudon *et al.*), *The Energy Calibration of LEP in 1992*, CERN SL/93-21 (DI), April 1993.

[12] Working group on LEP energy (R. Assmann *et al.*), Z. Phys. **C66** (1995) 567-582.

[13] Working group on LEP energy (R. Billen *et al.*), Eur. Phys. J. **C6** (1999) 187.

[14] G. Montagna, O. Nicrosini, G. Passarino, F. Piccinni and R. Pittau, Nucl. Phys. **B401** (1993) 3; Comp. Phys. Comm. **76** (1993) 328; Comp. Phys. Comm. **93** (1996) 120;
G. Montagna, O. Nicrosini, G. Passarino and F. Piccinini, hep-ph/9804211, recently updated to include initial state pair radiation (G. Passarino, priv. comm.).

[15] D. Bardin *et al.*, Z. Phys. **C44** (1989) 493;
Comp. Phys. Comm. **59** (1990) 303;
Nucl. Phys. **B351** (1991) 1;
Phys. Lett. **B255** (1991) 290 and CERN-TH 6443/92 (May 1992);
DESY Report 99-070, hep-ph/9908433 (Aug. 1999); recently updated with results from [17], accepted for publication by Comp. Phys. Comm.

[16] D. Bardin, G. Passarino, *Upgrading of Precision Calculations for Electroweak Observables*, hep-ph/9803425 ;
D. Bardin, G. Passarino and M. Grünewald, *Precision Calculation Project Report*, hep-ph/9902452 .

[17] A.B. Arbuzov, *Light pair corrections to electron-positron annihilation at LEP/SLC*, hep-ph/9907500.

[18] T. van Ritberben, R. Stuart, Phys. Lett. **B437** (1998) 201;
Phys. Rev. Lett. **82** (1999) 488.

[19] S. Eidelmann and F. Jegerlehner, Z. Phys. **C67** (1995) 585;
M. Steinhauser, Phys. Lett. **B249** (1998) 158.

[20] Particle Data Group (C. Caso *et al.*), Eur. Phys. J. **C3** (1998) 1.

[21] Particle Data Group (D.E. Groom *et al.*), Eur. Phys. J. **C15** (2000) 1.

[22] W. Beenakker, F.A. Berends and S.C.van der Marck, Nucl. Phys. **B349** (1991) 323.

[23] W. Beenakker and G. Passarino, Phys. Letters **B425** (1998) 199.

[24] W. Beenakker and G. Passarino, private communications.

[25] S. Jadach *et al.*, BHLUMI 4.04, Comp. Phys. Comm. **102** (1997) 229;
S. Jadach and O. Nicrosini, *Event generators for Bhabha scattering*, in *Physics at LEP2*, CERN 96-01 Vol. 2, February 1996.

[26] B.F.L. Ward, S. Jadach, M. Melles, S.A. Yost, Phys. Lett. **B 450** (1999) 262.

[27] G. Montagna *et al.*, Nucl. Phys. **B547** (1999) 39; Phys. Lett. **B459** (1999) 649.

[28] F.A. Berends, W.L. van Neerven and G.J.H. Burgers, Nucl. Phys. **B297** (1988) 429 and **B304** (1988) 921.

[29] E.A. Kuraev and V.S.Fadin, Sov. J. Nucl. Phys. **41** (1985) 466.

[30] G. Montagna, O. Nicrosini and F. Piccinini, Phys. Lett. **B406** (1997) 243.

[31] M. Skrzypek, Acta Phys. Polonica, **B23** (1992) 135.

[32] S. Jadach, M. Skrzypek and B.F.L. Ward, Phys. Lett. **B257** (1991) 173.

[33] D.R. Yennie, S.C. Frautschi and H. Suura, Ann. Phys. (NY) **13** (1961) 379.

[34] S.Jadach, B.Pietrzyk and M. Skrzypek, Phys. Lett. **B456** (1999) 77.

[35] L. Garrido *et al.*, Z. Phys. **C49** (1991) 645;
M. Martinez and F. Teubert, Z. Phys. **C65** (1995) 267, updated with results summarized in [34] and [48].

[36] S. Jadach, B. Pietrzyk, E. Tournefier, B.F.L. Ward and Z. Wąs, Phys. Lett. **B465** (1999) 254.

[37] B.A. Kniehl *et al.*, Phys. Lett. **B 209** (1988) 337.

[38] S. Jadach, M. Skrzypek and M. Martinez, Phys. Lett. **B280** (1992) 129.

[39] A. Leike, T. Riemann, J. Rose, Phys. Lett. **B273** (1991) 513;
T. Riemann, Phys. Lett. **B293** (1992) 451;
S. Kirsch, T. Riemann, Comp. Phys. Comm. **88** (1995) 89.

[40] The TOPAZ Collaboration (K. Miyabayashi *et al.*), Phys. Lett **B347** (1995) 171.

[41] The VENUS Collaboration (K. Yusa *et al.*), Phys. Lett. **B447** (1999) 167.

[42] ALEPH Collaboration (D. Busculic *et al.*), Z. Phys. **C 71** (1996) 179.

[43] DELPHI Collaboration (P. Abreu *et al.*), Eur. Phys. J. **C11** (1999) 383.

[44] L3 Collaboration (O. Adriani *et al.*), Phys. Lett. **B 315** (1993) 637;
L3 Collaboration (M. Acciarri *et al.*), Phys. Lett. **B 479** (2000) 101;
Phys. Lett. **B 489** (2000) 93.

[45] OPAL Collaboration (K. Ackerstaff *et al.*), Eur. Phys. J. **C2** (1998) 441.

[46] M. Veltman, Nucl. Phys. **B 123** (1977) 89.

[47] SLD Collaboration (K. Abe *et al.*), Phys. Rev. Lett. **84** (2000) 5945.

[48] *Reports of the working group on precision calculations for the Z resonance*, CERN 95-03, ed. D. Bardin, W. Hollik and G. Passarino, and references therein.